A three-dimensional study of the tropospheric sulfur cycle

M. Pham,[1] J.-F. Müller,[2] G. P. Brasseur,[3] C. Granier,[3] and G. Mégie[1]

Abstract. The global tropospheric distributions of seven important sulfur species were simulated with a global three-dimensional chemistry-transport model (IMAGES). Surface emission and deposition velocity maps were established for use as lower boundary conditions in the model. While anthropogenic SO_2 emissions are by far the largest sulfur source in the northern midlatitudes, reduced sulfur compounds, notably dimethyl sulfide (DMS) predominate over most remote areas. Simulations were performed for the present-day ($\sim$ 1985) atmosphere. The calculated distributions are compared with available observations. The model results are found to be generally within a factor of (at most) 2-3 of long-term observations. Comparison with campaign measurements is more difficult, mostly due to the strong dependence of sulfur species concentrations on local meteorological conditions. The results, however, indicate the need for future model refinements, especially with respect to biogenic emission estimates and parameterization of cloud processes. A sensitivity study is presented to discuss the uncertainties of the results related to several parameters (the decoupling of wet scavenging and convective transport for soluble species, volcanoes emission and deposition velocities). Results are also discussed in terms of global budgets and related variables and processes. Around 125 Tg S/yr of non-sea-salt (nss) sulfur compounds (DMS, CS_2, H_2S, COS, and SO_2) are injected into the atmosphere. The balance is mainly maintained by nss-sulfates wet and dry deposition, and by SO_2 dry deposition (94% of total sulfur deposition). It is found that DMS oxidation represents the main contribution to SO_2 chemical production (80% of the chemical sources), and that the major sink of SO_2 is provided by in-cloud oxidation (90% of the chemical sinks), under the assumption that all SO_2 incorporated into clouds is oxidized. The calculated annual wet deposition of sulfates reaches 3 g S m^{-2} yr^{-1} over Europe and North America, while it is usually lower than 0.5 g S m^{-2} yr^{-1} in remote parts of the world. Estimations for the global lifetimes are 0.9 day for DMS, 4 days for CS_2, 2.2 days for H_2S, 0.6 day for SO_2, 0.18 day for DMSO, 6.1 days for MSA, and 4.7 days for nss-sulfates.

1. Introduction

The sulfur cycle is known to have an important impact on the environment and the climate. Since the first studies of smog photochemical formation in the 1950s, the effect of man-made activities on our environment has been a growing matter of concern and the role of sulfur oxides on the acidification of lakes and forests has been stressed [OECD, 1977]. Sulfur gases are also known to be precursors to sulfate aerosols and CCN

[1]Service d'Aéronomie du CNRS, Paris, France.

[2]Belgian Institute for Space Aeronomy, Brussels, Belgium.

[3]National Center for Atmospheric Research, Boulder, Colorado.

(cloud condensation nuclei), and can affect the climate by backscattering solar radiation and by changing the albedo of clouds [Charlson et al., 1992]. In that sense, they could reduce the impact of greenhouse gases in the global mean and should therefore be considered in any assessment of future climate changes. Moreover, carbonyl sulfide (COS) and sulfur dioxide (SO_2) are the main precursors of the stratospheric sulfate aerosol layer, which might affect significantly the ozone budget and the Earth's radiation balance.

The need for quantifying these effects requires the development and use of models describing the global distributions of sulfur compounds with their emission fluxes, transport, and chemistry. Sulfur gases have both natural and anthropogenic sources, which are highly variable in time and space : oceans are the main source of biogenic sulfur compounds (mainly as dimethyl sulfide DMS), while SO_2 is mostly emitted as a result of human activities over continental industrialized areas [Spiro et al., 1992]. A three-dimensional model is therefore necessary to assess the relative importance of

anthropogenic and natural sources affecting the sulfur cycle.

Three-dimensional model studies of tropospheric sulfur have been reported earlier. *Erickson et al.* [1991] used a Lagrangian model to derive the global distribution of CCNs from DMS and SO$_2$ oxidation, on the basis of a very simple chemical scheme. A simplified treatment of the conversion of SO$_2$ into sulfates was also used by *Luecken et al.* [1991] with an Eulerian model. The meteorological fields used in both studies were derived from a general circulation model (GCM). *Langner and Rodhe* [1991] investigated the budget and distributions of DMS, SO$_2$, and nss-sulfates (nss SO$_4^{2-}$), using the chemistry-transport MO-GUNTIA model, which includes the detailed chemistry of 15 species and uses monthly mean winds from the climatology of *Oort* [1983]. The horizontal resolution of this model is $10^o \times 10^o$, with 10 levels in the vertical. In the present study, the tropospheric sulfur cycle is simulated with a comprehensive global three-dimensional chemistry-transport model, named IMAGES (Intermediate Model for the Annual and Global Evolution of Species) [*Müller and Brasseur*, 1994]. Seven sulfur compounds are considered in the model, namely, dimethylsulfide (DMS), hydrogen sulfide (H$_2$S), carbon disulfide (CS$_2$), sulfur dioxide (SO$_2$), dimethylsulfoxide (DMSO), methanesulfonic acid (MSA) and non-sea-salt sulfates (nss SO$_4^{2-}$). The general features of the model will be briefly described in section 2. Sulfur emission maps have been established and are presented in section 3. Section 4 presents the main physico-chemical reactions in the sulfur cycle and their parameterization in the IMAGES model. Results are discussed in sections 5 and 6 in terms of global distributions, seasonal variations and global budgets.

2. General Description of IMAGES

The chemistry-transport model IMAGES calculates the three-dimensional distribution and the global budget of the most important chemically active trace gases in the troposphere [*Müller*, 1993; *Müller and Brasseur*, 1994], including oxygen, hydrogen, and nitrogen compounds, as well as six hydrocarbons and their oxidation products. This model extends from the Earth's surface to the lower stratosphere and includes 25 altitude levels, 10 of them in the planetary boundary layer, the first level being located at about 35 m, the last one at 50 hPa. The horizontal resolution is 5 degrees in longitude as well as in latitude. Emission inventories for several types of emissions and compounds were developed by *Müller* [1992] and used as lower boundary conditions. The model includes about 130 chemical and photochemical reactions describing the sources and sinks of approximately 40 species, before sulfur compounds and related processes were introduced. Surface deposition of chemical compounds as well as wet removal of water soluble species are taken into account. The species whose lifetime is larger than several hours are transported by winds, diffusion, and cloud convec-

tion. This is the case for all sulfur compounds considered in the model. In this "intermediate model" the advective transport is based on monthly mean winds, and the effect of the wind variability during a given month is accounted for through an additional diffusion approach, in which the eddy diffusion coefficient is a function of the variance in the wind (see *Müller and Brasseur* [1994] for further details). The three-dimensional winds used in the IMAGES model, as well as the surface pressure, the temperature, and water vapor fields are average fields (1985-1989) derived from a global analysis of European Centre for Medium-Range Weather Forecasts (ECMWF) fields [*Trenberth and Olson*, 1988]. The cloud data were extracted from the International Satellite Cloud Climatology Project (IS-CCP) database and averaged over the period 1984-1987 (further details are given in paragraph 5). The precipitation fields, on the other hand, are climatological values based on the study of *Shea* [1986], corresponding to the period 1950-1979. The use of averaged data on relatively long periods guarantees a broad consistency of the model inputs and allows the model to provide slow-varying concentrations that can be compared with climatological averages. The distribution of atmospheric species is given by the mass conservation equation

$$\frac{\partial \rho_i}{\partial t} + \nabla(\rho_i \vec{V}) = P_i - S_i, \qquad (1)$$

where ρ_i stands for density of compound i, $\vec{V}$ is the wind vector, t is time, and P_i and S_i are the production (chemistry, emission term in the atmosphere, ...) and destruction (chemistry, wet removal, ...) terms. The short-lived species are not transported in the model; that is, the second term of the left-hand-side of (1) is neglected. For the other species, this term is decomposed into advection, diffusion, and cloud convection contributions. Here (1) is solved numerically by a time-splitting method. Advection is addressed using a semi-Lagrangian scheme, as described in *Müller and Brasseur* [1994]. Significant errors are known to be associated with diurnal mean concentrations calculated with fixed averaged photodissociation coefficients [*Turco and Whitten*, 1978]. In order to represent the diurnal variation of the chemical compounds without prohibitive computer cost, the model is integrated with a time step of 30 min during the first 3 days of each month and 1 day for the remaining of the month. During these later periods, the diurnal variation is accounted for on the basis of the diurnal variation calculated during the third day of each month. The model results were evaluated by comparisons with observations, including measurements of ozone, nitrogen oxides and carbon monoxide [*Müller*, 1993, *Müller and Brasseur*, 1994]. The chemical lifetime of methane ($\sim$ 10 years) is in good agreement with previous estimates, suggesting that hydroxyl (OH) concentrations are calculated accurately. The model is integrated during 2 years and the results are presented for the second year of simulation, when all compounds (CH$_4$, CO, O$_3$, NO$_x$, ...) are known to be close to steady state. A 1-year integration requires ap-

proximately 12 hours CPU time on 1 processor of the National Center for Atmospheric Research supercomputer CRAY Y-MP.

3. Earth-Atmosphere Interface: Emission Maps and Deposition Velocities

If the release in the atmosphere of man-made gaseous sulfur compounds is relatively well quantified (at least in industrialized countries), large uncertainties remain about the natural sources, in particular, by the ocean and the tropical biosphere. In order to assess the variability of sulfur compounds concentrations in the atmosphere, an inventory of sulfur emissions has been established and the resulting values have been used as lower boundary conditions in the model. All the emission maps presented here were calculated using the world ecosystem database established by *Olson et al.* [1985], and the soil database established by *Zobler* [1986]. Emission maps on the model surface grid (5° × 5°) were derived for each month of the year, and hence account for the seasonal variation of the sulfur emissions.

3.1. Anthropogenic Sources

Anthropogenic emissions are currently the most important source of gaseous sulfur compounds in the atmosphere. Anthropogenic sources include fossil fuel combustion, coal refining, and ore smelting in the case of SO_2 [*Hameed and Dignon*, 1988], and automobiles, chemical industries, sulfur recovery processes in the case of COS and CS_2 [*Khalil and Rasmussen*, 1984]. The inventory of anthropogenic emissions of SO_x has been taken from *Müller* [1992]. The emission fluxes for countries of the Organization of Economic Cooperation and Development (OECD) are those compiled by *OECD* [1989]. The emissions for the other countries were estimated from the industry and energy statistics of the United Nations [*UN*, 1986]. *Müller* [1992] estimated a global source strength of 92 Tg S/yr (cf. Table 1), which is well in the range of other published estimates, such as *Spiro et al.* [1992] (77 Tg S/yr), and *Cullis and Hirschler* [1980] (103.6 Tg S/yr). Further comparison with *Spiro et al.* [1992] indicates that the

study of *Müller* [1992] predicts larger emission rates in the northern midlatitudes (around 40% on average) and lower values in the Arctic due to an underestimation of the smelting activities at Norilsk (Siberia). The discrepancies are also due to differences in the assumed emission factors and the use by *Spiro et al.* [1992] of other emission data for some parts of the world, such as the former Soviet Union.

We assumed that all man-made SO_x was emitted as SO_2, although a small fraction of the source (no more than about 5%) might be direct emission of sulfates [*Langner and Rodhe*, 1991, *EMEP*, 1989]. Using the global anthropogenic source strengths of COS and CS_2 estimated by *Khalil and Rasmussen* [1984], (respectively 0.07 Tg S/yr and 0.3 Tg S/yr), emission maps for these compounds were derived from the SO_2 maps, using the molar emission ratios $COS/SO_2 = 8 \times 10^{-4}$ and $CS_2/SO_2 = 3 \times 10^{-3}$.

3.2. Biogenic Sources

Oceans. In open ocean waters, DMS is the main sulfur compound emitted to the atmosphere. It is known to be produced by zooplanctonic grazing and phytoplanctonic senescence [*Nguyen et al.*, 1988]. There is, however, no simple correlation between chlorophyll concentration and ocean DMS concentration as the production of this molecule is very species-specific [*Nguyen et al.*, 1990]. For this reason, we considered the empirical solar radiation DMS flux relationship of *Bates et al.* [1987] to derive the distribution of DMS emissions: we chose a global source strength of 19.2 Tg S/year of DMS, which is in the range of previous estimates by *Andreae and Raemdonck* [1983], *Galloway* [1985], *Andreae* [1986] (32-35 Tg S/yr), *Bates et al.* [1992] (16 ± 11 Tg S/yr), *Cooper and Saltzmann* [1991] (6-10 Tg S/yr), and *Spiro et al.* [1992] (9.4-11.9 Tg S/yr). This total was then distributed over the world oceans and modulated with the solar flux reaching the ocean, according to *Bates et al.* [1987] (cf. Table 1). The solar flux was computed with the radiative model of *Madronich* [1987] with cloud cover and optical depth distributions derived from ISCCP (see section 4). This method neglects the spatial distribution of chlorophyll and therefore underestimates the flux in areas associated with high productivity. Comparison with measurements by *Bates et al.* [1990b] indicates an underestimation of the

Table 1. Estimated Global Emissions of Sulfur Species

Sources	SO_2	H_2S	COS	DMS	CS_2	Total
Volcanoes	9.2					9.2
Biosphere		0.52	0.35	0.31	0.0064	1.18
vegetation		0.5	0.21	0.29	0.004	1
soils		0.02	0.14	0.02	0.0024	0.18
Biomass burning	2.9		0.11			3
Ocean			0.3	19.2	0.2	19.7
Man-made	92		0.07		0.3	92.4
Total	104.1	0.52	0.83	19.5	0.5	125.5

Emissions are in teragrams sulfur per year.

DMS emission rates by a factor 2-3 in the coastal areas of the latitudinal band $0°$-$20°$N.

Oceans are also an important source of COS and CS_2, whose fluxes are estimated to be 1-2% of the DMS flux [*Bates et al.*, 1992]. Though COS is produced by the photooxidation of organic matter [*Ferek and Andreae*, 1984], the seasonal and geographical variations of COS and DMS are similar at the model scale. Thus COS and CS_2 oceanic emission rates can be assumed proportional to DMS emission rates. The global COS source strength is around 0.3 Tg S/yr, according to published estimates [*Johnson and Harrison*, 1986 (0.2-0.4 Tg S/yr); *Andreae*, 1986 (0.35 Tg S/yr); *Khalil and Rasmussen*, 1984 (0.32 Tg S/yr); *Andreae and Ferek*, 1992; (0.41 Tg S/yr)]. The adopted global source of CS_2 is 0.2 Tg S/yr, as estimated by *Andreae* [1986].

Continental biosphere. Sulfur is an essential element for plant growth. It can be directly volatilized by leaves of living plants and emitted by soils as a result of organic matter decomposition and biological transformation in soils. Measurement data of sulfur fluxes from the soil/vegetation system are not as numerous as those from the oceans (especially in the tropics). These emissions are particularly difficult to quantify as they are affected by as many factors such as temperature, tidal flushing, availability of sulfur, soil moisture, soil pH, mineral composition ground cover, and solar radiation [*Guenther et al.*, 1989].

The release and uptake mechanisms of sulfur are not only poorly known, but are also extremely variable, even at a given site and a given period [*Castro and Galloway*, 1991; *Aneja*, 1990]. Hence in a first approximation, biospheric emission maps used in this work are based on the inventory developed by *Guenther et al.* [1989] for the United States, using temperature dependent emission algorithms and available biomass, land use, and climatic data. The *Guenther et al.* [1989] estimates of COS, CS_2, DMS, and H_2S fluxes for different types of soils and vegetation in the United States were extrapolated over the entire world, except in the more productive tropical regions where the values of *Andreae and Andreae* [1988a] and *Andreae et al.* [1990] were distributed over the tropical forest and soil ecosystems. Our global annual estimates are summarized in Table 1 for the soil and vegetation ecosystems and for COS, CS_2, DMS, and H_2S, respectively. The total estimated source strength is 1.18 Tg S/yr. This value is about 3 times higher than the estimate by *Bates et al.* [1992]. However, the emission algorithm used by these authors seems to underestimate the observed emission rates in the Tropics by *Andreae and Andreae* [1988a] and *Andreae et al.* [1990]. Because of the model scale and the flux uncertainties, the adopted methodology has been chosen to be as simple as possible, and could certainly be improved with additional measurements and a better understanding of emission mechanisms.

Biomass burning. Biomass burning also contributes to the emission of sulfur compounds (mostly as COS and SO_2) in the atmosphere since plants contain around 0.1-0.25% of sulfur, of which 40-50% is released

during the fires [*Delmas*, 1982]. Using the global data of *Müller* [1992] for CO_2 emissions by biomass burning, emission maps were inferred using values of 3×10^{-4} for the SO_2/CO_2 molar emission ratio [*Delmas and Servant*, 1983] and 1.2×10^{-5} for the COS/CO_2 molar emission ratio [*Crutzen et al.*, 1979]. The global source strength calculated for both compounds is 3 Tg S/yr (Table 1), which is within the range of estimates by *Andreae and Andreae* [1988a] and *Andreae et al.* [1990] (2 Tg S/yr), *Delmas and Servant* [1983] (3.5 Tg S/yr), and *Spiro et al.* [1992] (2.3 Tg S/yr). The difference with the latter study is partly due to the larger global source strength of CO_2 in our study (3140 Tg C/yr versus 2860 Tg C/yr in *Spiro et al.* [1992]).

Volcanoes. Large volcanic eruptions affect the climate of the Earth and the chemistry of the atmosphere. The recent eruption of Mount Pinatubo injected about approximately 20 Mt of sulfur into the atmosphere (mostly in the stratosphere) [*Bluth et al.*, 1992]. During noneruptive periods, sulfur compounds (mainly SO_2) are also degassed by volcanoes. In order to take into account the volcanic emissions in a "climatological sense", we have used the volcanoes inventory by *Simkin et al.* [1981] and the Volcanic Explosivity Index (VEI) classification of *Newhall and Self* [1982]. The VEI defines the magnitude scale of an eruption. Global data on the locations, injection altitudes, and VEIs of well-documented active volcanoes in the last thousand years were considered in our emission maps. As a first step, the episodic character of eruptions has not been taken into account. All volcanoes were therefore assumed to inject sulfur continuously into the atmosphere, depending on their noneruptive character or their VEI. Source strengths for each category are taken from *Stoiber et al.* [1987]. 3.4 Tg S/yr is assumed to be uniformly emitted by degassing volcanoes between 1 and 2 km. For volcanoes with VEI between 0 and 4, 5.1 Tg S/yr is distributed between 2 km and the tropopause with a constant rate. Volcanoes with VEI above 4 are assumed to inject 0.7 Tg S/yr into the stratosphere. Comparison with *Spiro et al.* [1992] who used a more detailed methodology in terms of injection height and temporal variations, shows an agreement within a factor less than 2 with their zonally 9-year-averaged data. Our methodology provides a relatively high estimate of the emissions associated with eruptive volcanoes, which explains the differences between the *Spiro et al.* [1992] estimate (7.8 Tg S/yr) and ours (9.2 Tg S/yr) (see Table 1).

Table 1 gives as a summary the yearly globally integrated fluxes for each sulfur compound and each source. Anthropogenic activities represent the major source of sulfur compounds (76%, if we include biomass burning) and they are known with an uncertainty of $\pm$50% (biomass burning included). Among the biogenic sources, oceans contribute to 16% of the total source, DMS being the main compound emitted. These sources represent the major uncertainty in the estimates, mainly due to the uncertainties in the emission of DMS by the oceans and the emission of H_2S by the tropical biosphere.

a/

b/
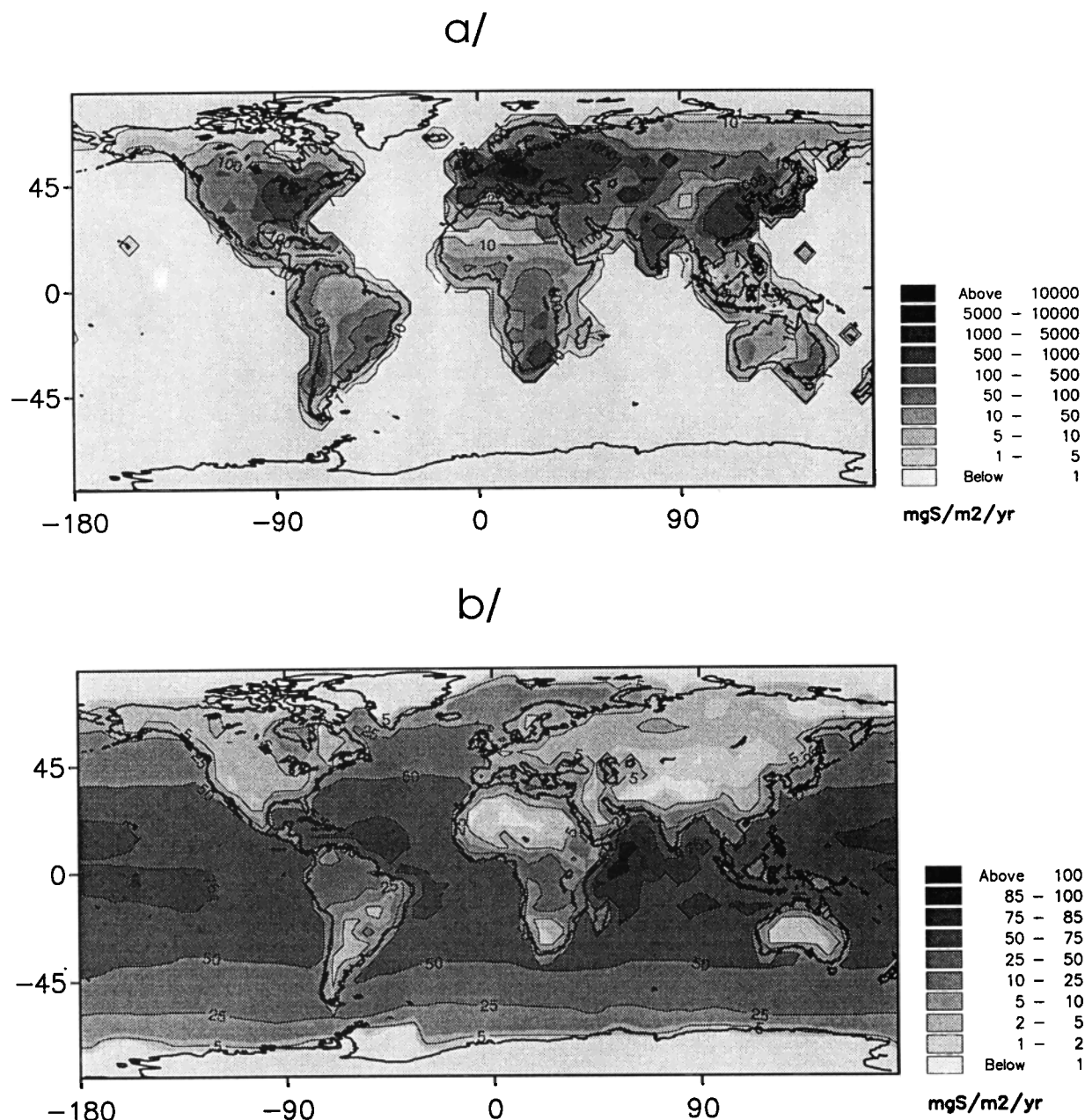
Figure 1. Annual total sulfur emission rates in mg S m^{-2} yr^{-1}, (a) anthropogenic emissions only (including biomass burning), (b) biogenic emissions only.

As shown in Figures 1a and 1b, which illustrate the annually averaged distributions of anthropogenic and biogenic rates, respectively, values related to the sources of human origin sometimes exceed the biogenic emission rates by 1 to 3 orders of magnitude. The anthropogenic man-made sources are localized in Europe, Eastern North America, the Far East (because of fossil fuel combustion), Africa and South America (due to ore smelting), and in the tropics (biomass burning). They are concentrated in the northern hemisphere, while biogenic emissions are predominant in the southern hemisphere. Emissions by the continental biosphere are mainly localized over the Tropics. The corresponding emission rates of DMS and H$_2$S are of the same order

of magnitude as oceanic DMS rates. The continental rates are otherwise much smaller than the oceanic rates and, in the northern hemisphere, they represent less than 1% of the total source. This geographic variability of the emission rates confirms the necessity of using a three-dimensional model to study the global sulfur cycle.

Besides the processes of emissions at the Earth-atmosphere interface, deposition velocities were prescribed according to several authors for COS [*Taylor et al.*, 1983; *Goldan et al.*, 1987; *Mihalopoulos et al.*, 1989], DMSO [*Chatfield and Crutzen*, 1984], SO$_2$ [*Galloway*, 1985], MSA and the nss-sulfates (values based on the inventory by *Voldner et al.* [1986]). The deposition ve-

locities are corrected in the model to account for the aerodynamic resistance occurring between the surface and the first level as described in *Müller and Brasseur* [1994]. They are assumed to be constant, except that they differ for ocean and continents (see Table 2). We acknowledge that this is a crude estimate, which needs to be refined in the future. The sensitivity of the model results to this parameter is discussed in section 5.8.
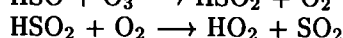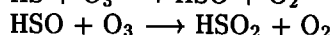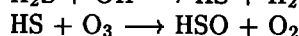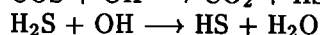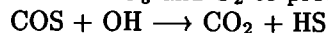
4. Production and Destruction in the Troposphere

Once emitted in the atmosphere, sulfur compounds and their subsequent oxidation products are transported and/or chemically converted, mainly by OH (daytime) and NO_3 radicals (nighttime), before being removed by wet and dry deposition. The main oxidation products are DMSO, SO_2, $DMSO_2$ (dimethyl sulfone), MSA, and H_2SO_4. $DMSO_2$ is neglected in our mechanism, since its concentration is believed to be small relative to that of other species [*Harvey and Lang*, 1986]. The acid vapors MSA and H_2SO_4 are known to condense on preexisting particles and/or to generate new particles through nucleation in the H_2O/MSA/H_2SO_4 system, under favorable conditions of temperature and relative humidity [*Jaecker-Voirol and Mirabel*, 1988, *Hoppel*, 1987]. In the troposphere, they form particles in a few minutes [*Kreidenweis and Seinfeld*, 1988], so that they are considered as aerosols in the model.
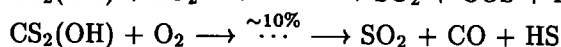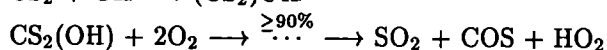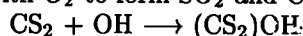
4.1. Gas Phase Chemistry

The gas phase reactions and rates adopted in the model are presented in Table 2. As COS is distributed in the atmosphere with a nearly uniform concentration of approximately 500 parts per trillion by volume

(pptv) (due to its long lifetime of about 2 years), we adopted a constant COS profile for our calculations. In this section, we describe in more details the mechanisms and related uncertainties of sulfur gas phase chemistry. The gas phase chemical mechanisms for the oxidation of COS, H_2S, CS_2, and SO_2 with OH are relatively well known [*Tyndall and Ravishankara*, 1991], although uncertainties remain concerning for example the products of the reaction CS_2 + OH.
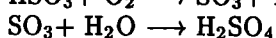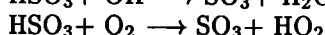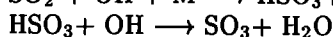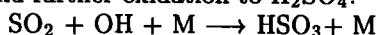
The oxidation of COS and H_2S with OH results in the production of the intermediate product HS, which reacts with O_3 and O_2 to produce SO_2

$$COS + OH \longrightarrow CO_2 + HS$$
$$H_2S + OH \longrightarrow HS + H_2O$$
$$HS + O_3 \longrightarrow HSO + O_2$$
$$HSO + O_3 \longrightarrow HSO_2 + O_2$$
$$HSO_2 + O_2 \longrightarrow HO_2 + SO_2$$

The reaction CS_2+OH proceeds through an addition mechanism, the intermediate adduct CS_2(OH) reacting with O_2 to form SO_2 and COS with a 90% efficiency

$$CS_2 + OH \longrightarrow (CS_2)OH$$
$$CS_2(OH) + 2O_2 \xrightarrow{\geq 90\%} \cdots \longrightarrow SO_2 + COS + HO_2$$
$$CS_2(OH) + O_2 \xrightarrow{\sim 10\%} \cdots \longrightarrow SO_2 + CO + HS$$

The oxidation of SO_2 is a three-body reaction with a rate determining step resulting in the HSO_3 radical, and further oxidation to H_2SO_4.

$$SO_2 + OH + M \longrightarrow HSO_3 + M$$
$$HSO_3 + OH \longrightarrow SO_3 + H_2O$$
$$HSO_3 + O_2 \longrightarrow SO_3 + HO_2$$
$$SO_3 + H_2O \longrightarrow H_2SO_4$$

The oxidation mechanism for DMS under atmospheric conditions is not yet completely elucidated, due in part to the difficulty in conducting experiments at the

Table 2. Chemical Rate Coefficients and Prescribed Deposition Velocities

Reactions	Rate Coefficients $cm^3molec^{-1}s^{-1}$
OH + DMS → SO_2 + ...	$9.6 \times 10^{-12} \times \exp(-234/T)$
OH + DMS → 0.6 SO_2 + 0.4 DMSO + ...	$3.04 \times 10^{-12} \times \exp(350/T) \times \alpha/(1+\alpha)$
	with $\alpha = 1.106 \times 10^{-31} \times \exp(7460/T) \times M$
	M : air density (molecules/cm^3)
OH + DMSO → 0.6 SO_2 + 0.4 MSA + ...	5.8×10^{-11}
NO_3 + DMS → SO_2 + ...	$1.9 \times 10^{-13} \times \exp(500/T)$
OH + CS_2 → SO_2 + COS + ...	$8.8 \times 10^{-16} \times \exp(2300/T)$
OH + H_2S → SO_2 + ...	$6.0 \times 10^{-12} \times \exp(-75/T)$
OH + COS → SO_2 + ...	$1.1 \times 10^{-13} \times \exp(-1200/T)$
OH + SO_2 + M → sulfates + ...	$\alpha_0 \times M/(1 + \alpha_0 \times M/\alpha_\infty) \times 0.6^{(1./(1.+log_{10}(\alpha_0 \times M/\alpha_\infty)^2))}$
	with $\alpha_0 = 3 \times 10^{-31} \times (300/T)^{3.3}$
	and $\alpha_\infty = 1.5 \times 10^{-12}$

| Dry deposition | Velocity in cms^{-1} | |
	Ocean	Continent
SO_2	1.1	0.9
DMSO	1	0
MSA	0.5	0.5
sulfates	0.5	0.5

low atmospheric concentrations of the gas phase species [*Yin et al.*, 1986]. Kinetic studies show that 70% of the reaction proceeds through an abstraction pathway, while 30% of the products are due to an addition pathway [*Hynes et al.*, 1986]. These pathways are strongly temperature dependent with addition occurring preferentially at temperatures below 10°C. However, the yields of these pathways and the reaction products are uncertain. In the model, SO_2 is assumed to be the only product of the abstraction pathway. Following *Barnes et al.* [1988], we also assume that the addition pathway leads to DMSO and SO_2, and we do not take into account MSA production during the oxidation of DMS in presence of nitrogen oxides, since this mechanism is not well understood. Destruction of DMS by iodine oxide (IO) has been suggested by *Carlier* [1985] to explain the short DMS lifetime observed in the coastal areas, but recent kinetic studies suggest that this mechanism plays only a secondary role [*Maguin et al.*, 1991]. Photodissociation of COS, CS_2 and SO_2 are ignored, since these reactions occur only for wavelengths below 280 nm, and can therefore be neglected in the troposphere [*Molina et al.*, 1981; *Okabe*, 1978; *Calvert and Stockwell*, 1983].

4.2. Cloud-related Processes

Besides their role on the radiative budget and the dynamics of the atmosphere, clouds are known to influence significantly the chemistry of the troposphere [*Lelieveld and Crutzen*, 1991]. This is particularly the case for SO_2, whose main chemical sink is in-cloud oxidation by oxidants like O_3 and H_2O_2 [*Calvert et al.*, 1985]. Moreover, clouds and precipitation efficiently remove sulfur compounds like SO_2, nss-sulfates, MSA and DMSO from the troposphere. In order to be simulated with accuracy, these processes would require that the formation of precipitation and clouds and their interaction with chemical compounds be considered. However, many of the chemical aqueous processes are still poorly understood, so that these subgrid scale processes are treated in a climatological way and are parameterized.

For this purpose, we use the ISCCP database, which provides the monthly averaged cloud cover fraction, the optical depth and the pressure level of the cloud tops for seven different cloud types (cumulus and stratocumulus, stratus, altocumulus and altostratus, nimbostratus, cirrus, cumulonimbus, cirrostratus and cirrocumulus). These data are given on the global scale with a resolution of 2.5° by 2.5° and are available for the period 1983-1990. We use data averaged over the years 1984-1987, in order to avoid the spurious effects of changes due to the NOAA satellite replacement in 1983 and in 1988 [*Klein and Hartmann*, 1993]. The cloud data were interpolated at the model grid (5° by 5°). In the polar night areas, where data on the different cloud type coverages are lacking, we use the existing ISCCP statistics on low, middle, and high clouds. Moreover, each cloud type is assumed to be vertically uniform, extending from its base to its top with the same cover fraction. The base altitude is calculated by attributing to each

type of cloud an approximative base pressure defined according to *Rossow et al.* [1987]. Figures 2a and 2b illustrate the cumulus cover fractions in January and July as derived from the ISCCP cloud database. These values are assumed to be constant between their base pressure fixed at 900 hPa, and their top pressure given by the ISCCP, which roughly varies between 680 hPa at around 25° and 850 hPa near the polar areas. Like all low-level clouds, cumulus are mainly concentrated over oceans. They are particularly important over the depression belts of the subtropical areas and over the continents of the summer hemisphere, where convective processes are induced by the temperature contrast between ocean and land. We compared the zonally and annually averaged cloud cover fraction used in IMAGES with the NCAR data compiled by *Warren et al.* [1985]. The two distributions are rather similar in shape (except in the case of cumulus, where the more recent ISCCP data are characterized by a minimum in the equatorial zone), but they differ occasionally by up to a factor of 3 (Figure 3). Though we are aware of the uncertainties related to these quantities, the ISCCP database can be considered as more consistent than the NCAR data, since it is based on observations performed from an unique platform on the NOAA satellite.

Wet removal. Wet scavenging is parameterized as a first-order reaction rate (s^{-1}). We adopt the *Langner and Rodhe* [1991] parameterization based on the *Junge and Gustafson* [1957] model to represent sulfur compounds in-cloud scavenging. The removal rate ($1/\tau$) is given by

$$1/\tau(z) = \frac{\epsilon}{LWC(z)} \times R(z), \tag{2}$$

where ϵ describes the removal efficiency depending on the soluble species, LWC is the liquid water content of the rain-producing cloud (gm^{-3}) and R, the average rate of formation of precipitable liquid water ($gm^{-3}s^{-1}$), at a given altitude z.

R is calculated as

$$R(z) = P\frac{F(z)}{\int_0^{tropopause} F(z)dz} \tag{3}$$

with

$$F(z) = \frac{f_{Cb}(z)LWC_{Cb} + f_{Ns}(z)LWC_{Ns}}{f_{Cb}(z) + f_{Ns}(z)},$$

where P is the precipitation rate ($gm^{-2}s^{-1}$), LWC_{Cb} (LWC_{Ns}) and f_{Cb} (f_{Ns}) are respectively the cloud liquid water content and the cloud fraction of cumulonimbus (nimbostratus) at the altitude z. We adopted the *Langner and Rodhe* [1991] constant values of the ratio $\frac{\epsilon}{LWC} = 1.2$ m^3/g for aerosols and $\frac{\epsilon}{LWC} = 0.5$ m^3/g for gases, in (2). These values are in the middle of the range calculated by these authors. We used the *Lelieveld* [1990] liquid water contents for nimbostratus ($LWC_{Ns} = 0.6$ gm^{-3}) and cumulonimbus ($LWC_{Cb} = 1$ gm^{-3}) in (3). The cloud fractions f_{Cb} for cumulonimbus and f_{Ns} for nimbostratus are derived from the methodology described in the introduction of this section.
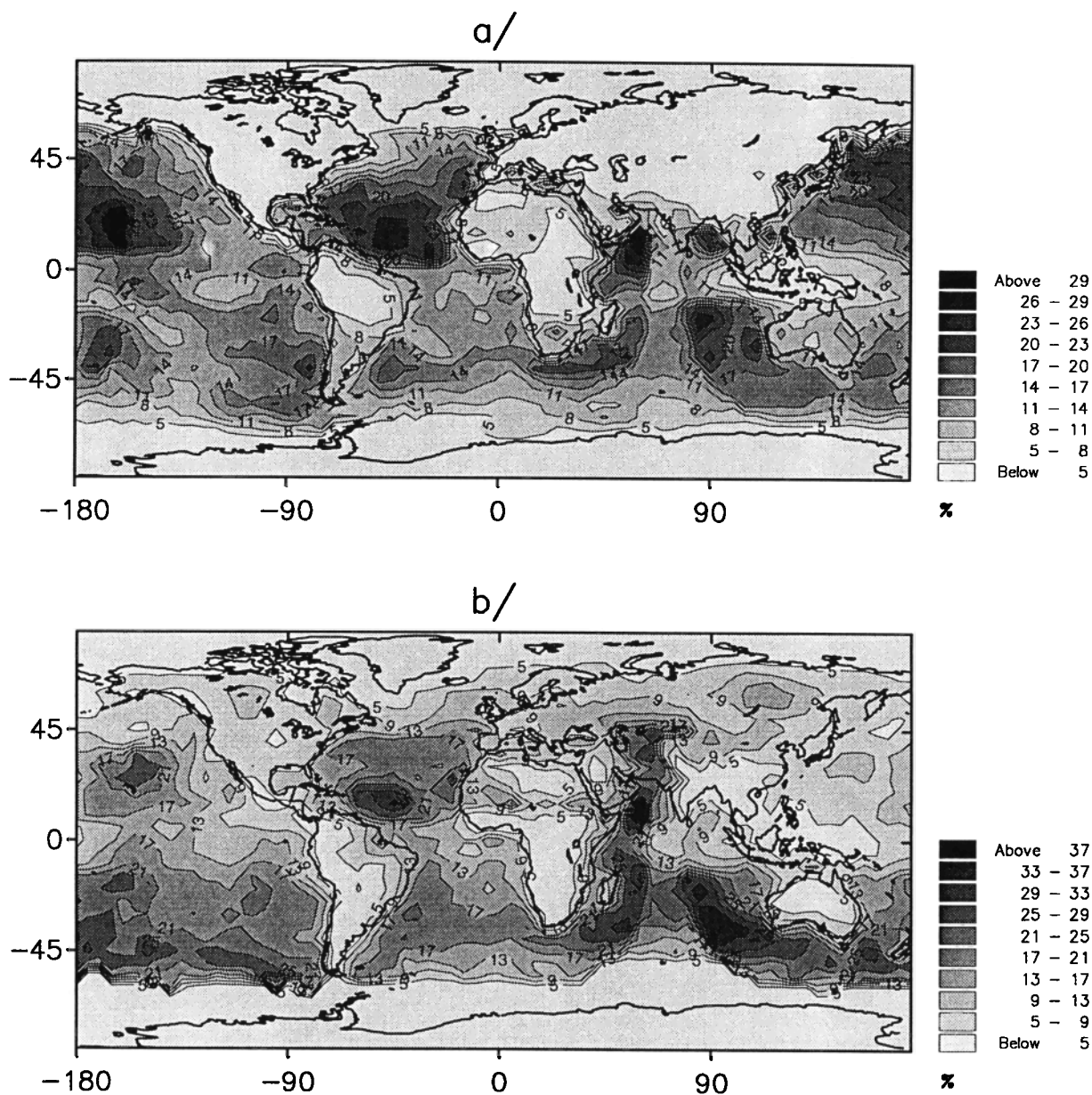
a/

b/

Figure 2. Cumulus cover fraction in percentage in (a) January and (b) July.

Sensitivity studies by *Chaumerliac et al.* [1987] show that in-cloud sulfate nucleation scavenging is 5 to more than 10 times stronger than below-cloud scavenging. Therefore, we only consider the in-cloud scavenging for the particles. For below-cloud scavenging of gases, we use the empirical relationship linking the scavenging rate $1/\tau$ (s^{-1}) to the precipitation rate P expressed in millimeters per hour according to *Martin* [1984]

$$\frac{1}{\tau} = 2.61 \times 10^{-5} \times P \qquad (4)$$

This value corresponds to a removal rate of 4.35×10^{-5} s^{-1} for a precipitation rate of 10 mm over 6 hours, which is within the range of the values used by the Co-operative Program for Monitoring and Evaluation of the Long Range Transmission of Air Pollutants in Europe

(EMEP) model [*Eliassen and Saltbones*, 1983; *Iversen et al.*, 1989].

We are aware of the fact that these approaches are preliminary and correspond to a climatological average: (4) was applied to SO$_2$ and DMSO irrespectively of the differences in their solubilities; this parameterization will be refined in the future. Besides, the calculated rate is assumed to be constant during the month. We do not take into account the episodic character of precipitation which leads to an increase in the lifetime of very soluble species [*Rodhe and Grandell*, 1972; *Giorgi and Chameides*, 1986; *Thompson and Cicerone*, 1982], nor did we consider the duration, intensity, or frequency of precipitation.

Aqueous-phase chemistry. In-cloud SO$_2$ oxidation mechanisms have been studied by several authors
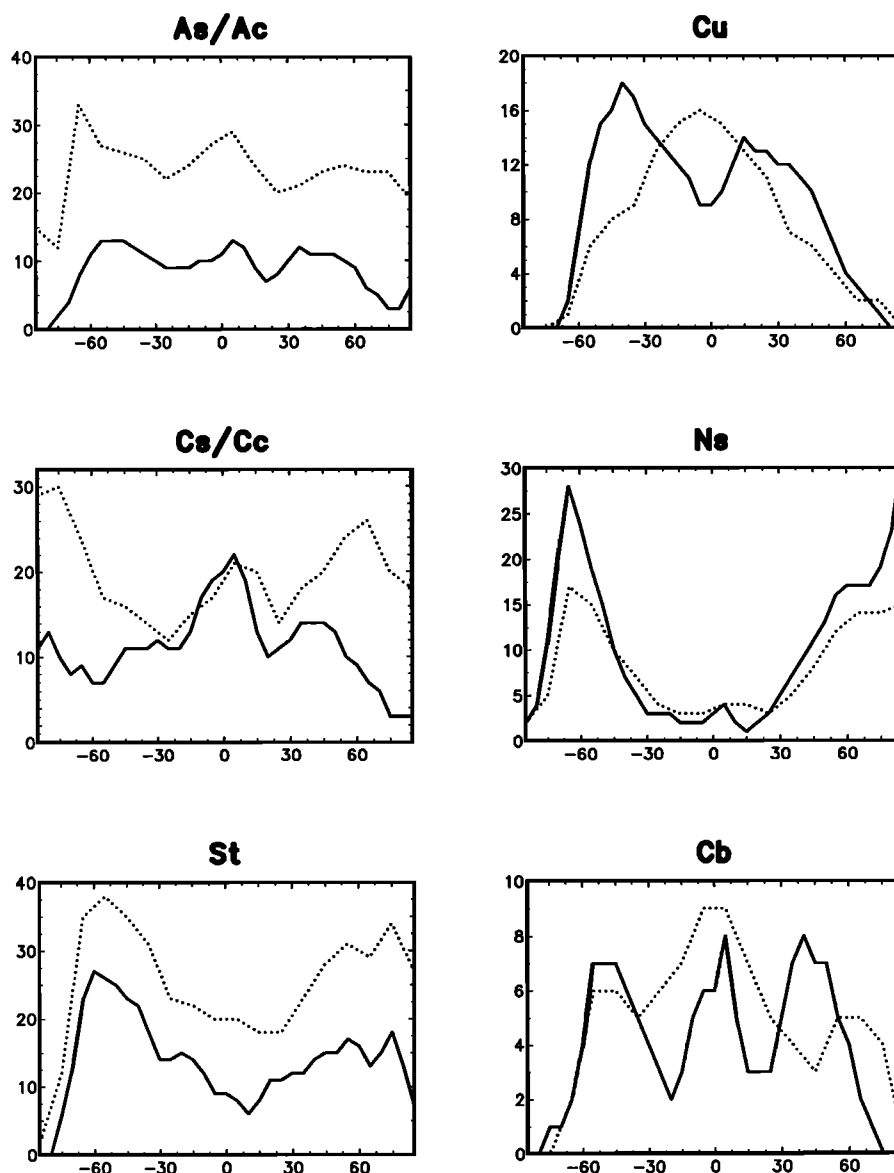
Figure 3. Zonally and annually averaged cover fractions of clouds derived from the ISCCP database (solid line) and NCAR database (dotted line). Notations are As/Ac for altostratus and altocumulus, Cu for cumulus, Cs/Cc for cirrostratus and cirrocumulus, Ns for Nimbostratus, St for stratus, Cb for cumulonimbus.

[*Hoffmann and Edwards*, 1975; *Penkett et al.*, 1979; *Martin and Damschen*, 1981; *Hoigné and Bader*, 1983]. When absorbed by cloud droplets, SO_2 partially dissolves and dissociates into HSO_3^- and SO_3^{2-}, before being oxidized to sulfates by H_2O_2 (for a cloud pH below 5) and by O_3 (higher pH). Dissolved SO_2 can also be oxidized by OH, HO_2, or O_2 in the presence of Mn^{2+} or Fe^{2+}. The modelling study of *Lelieveld* [1990] showed that in most cases, all sulfur IV is oxidized when a cloud is present. The average lifetime of SO_2 with respect to aqueous phase oxidation (τ_{aq}) is therefore determined by the cloud lifetime and the SO_2 in-cloud residence time, in a nonpolluted atmosphere. We refer to the parameterization of *Rodhe and Grandell* [1972] and *Langner and Rodhe* [1991] to compute τ_{aq} at a given altitude z

$$\tau_{aq}(z) = \tau_{nc}(z) \times (1 - f(z)), \qquad (5)$$

where f is the total cloud cover fraction ($f(z) = \sum_{i=1}^{7} f_i(z)$, where $f_i(z)$ is the monthly cover fraction of each cloud type i, at altitude z, derived at the model grid from the ISCCP database), and $\tau_{nc}(z)$ is the average time between two cloud occurrences. This latter value is inferred from $\tau_c(z)$, the average residence time of an air parcel inside a cloud, by

$$\tau_{nc}(z) = \tau_c(z) \times \frac{1 - f(z)}{f(z)} \qquad (6)$$

$$\tau_c(z) = \frac{\sum_{i=1}^{7} f_i(z)\tau_{c_i}}{\sum_{i=1}^{7} f_i(z)}, \qquad (7)$$

Table 3. Average Residence Time of an Air Parcel in a Cloud

| Cloud Types	Residence Time Used in the Model	*Lelieveld* [1990]
Cu	18 min	15-20 min
St	3 hrs	3-4 hrs
As/Ac	3 hrs	3 hrs
Ns	5.5 hrs	5.5 hrs
Cb	15 min	10-15 min

where the value of τ_{c_i}, the average residence time of an air parcel in a cloud of type i, is given in Table 3 for each type of cloud [*Lelieveld*, 1990]. Values for τ_{aq} range from 3 hours to more than 100 hours in areas of low cloud occurrence. Minimum values are localized between 800 hPa and 400 hPa with values depending on season, longitude, and latitude. They are usually lower over the depression belts at 60° and over the Intertropical Convergence Zone (ITCZ), with corresponding aqueous conversion times of 3-6 hours. At around 900 hPa, the lowest values (3-7 hours) are located over continents at around 30^oS and 45^oN in January, and 15^oN and 45^oN in July.

The parameterization adopted in the model neglects the dependence on O_3 and H_2O_2 concentrations. This might be not entirely appropriate in polluted areas, where SO_2 may exceed H_2O_2 and where the oxidation by ozone is less efficient because of the high acidity of the cloud droplets. Moreover, in these areas, catalytic reactions can be important. The box model calculations of *Lelieveld* [1990] suggest that the assumption that SO_2 is completely oxidized in each cloud event might be correct even for SO_2/H_2O_2 concentration ratios as large as 25, which is higher than our modelled values of this ratio in the regions where clouds are present. The calculations of this author do not cover all situations, so that this result might not be always valid, especially in winter above polluted areas. Since there is no simple parameterization of in-cloud conversion (besides an explicit calculation of aqueous chemistry), we did not take

into account in-cloud oxidant limitation, acknowledging that this represents a limitation of the model.

5. Results

In the following paragraphs, we will briefly describe the calculated three-dimensional distributions of sulfur compounds and compare them with existing data. The high reactivity of sulfur species and their resulting low concentrations in the atmosphere make the measurements of these species difficult. The spatial and temporal coverage of the measurements is thus far from adequate to accurately evaluate the model. Sulfur compounds are generally measured during localized campaigns or at a particular site for several months. In both cases, difficulties in comparing predicted concentrations with existing data arise from the spatial scale of the variability in the concentration of the sulfur compounds, as compared to the model resolution. Above remote areas or far away from sources of sulfur species, and in the high troposphere, where the residence time of the compounds is longer, the comparison seems more relevant. However, measured concentrations are strongly linked to local meteorological conditions, while simulated distributions are based on monthly averaged climatological data. In order to be consistent, the model should be driven by analysed winds, temperature, and pressure corresponding to the observed meteorological conditions, which is out of the scope of this study. The model results are thus better compared with monthly
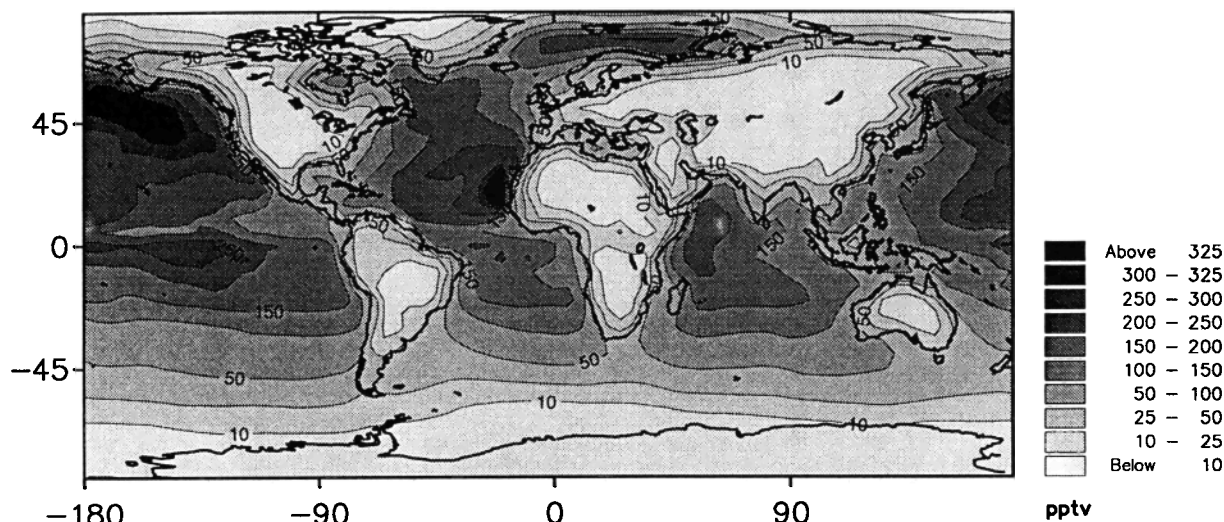
Figure 4. IMAGES DMS distribution at the surface in July.

Table 4. Measurements of DMS at Several Locations at the Surface, Unless Noted, and Comparison With Calculated Concentrations for the Same Areas and Time Periods

Location	Time Period	Mean (Median)	Range	Model	Ref
Bahamas	Nov	122 (70)	3 - 469	45	1
	June	154 (108)	25 - 300	129	2
Gulf of Mexico	Sept	25 (24)	5 - 70	108	2
Sargasso Sea	June	232 (115)	1 - 709	102	1
Caribbean	Feb/March	83 (57)	16 - 104	58-77	2
Barbados	June	70 ± 6		190	3
Bermuda	June		35 - 195	135	4
Atlantic					
- 40°N; 70-30°W	April/May	126	2 - 411	47 - 160	1
- 43°N-70°W	Jan/Feb		0.5 - 12	7	4
- 80°W-45°N	Jul/Aug	29 ± 25	1 - 110	57 - 104	5
- 65°W-45°N	August	101 ± 67	11 - 335	58	5
- 30-40°W	Oct		10 - 40	0.1 - 140	6
- 0-20°S					
Equatorial Pacific	July	168 (120)	47 - 289	274 (192 - 292)	1
- 90-180°W; ~ 0°					
	Nov	70	40 - 140	225	7
Tropical Pacific					
- 145-165°W; 15°S-20°N	Feb/March	347	272 - 446	234	11
- 170°W; 10°S-15°N	April/May	277 ± 178	57 - 647	236	16
Northeast Pacific	May		25 - 250	71	8
Northeast Pacific	May		0.6 - 30	71	9
Cape Grim	January	167 (130)	24 - 336	144	1
Antarctic	April	106 ± 55	17 - 236	86 (76 - 160)	10
Amazon Basin	Dry season				12
- surface		16 ± 10		22	
- mixed layer		9.1 ± 6.7		12	
- free troposphere		1.1 ± 0.8		1.4	
Amazon Basin	Wet season				13
- surface		16 ± 10		37	
- mixed layer		7.2 ± 3.1		26	
- free troposphere		0.9 ± 0.5		6	
Congo	Feb/March	30	7 - 75	69	14
Georgia	Jul/Sep		5 - 15	6.5	15

Concentrations are in parts per trillion by volume.
References : 1, *Andreae et al.* [1985b]; 2, *Saltzmann and Cooper* [1988]; 3, *Ferek et al.* [1986]; 4, *Van Valin et al.* [1987]; 5, *Cooper and Saltzmann* [1991]; 6, *Barnard et al.* [1982]; 7, *Nguyen et al.* [1984]; 8, *Bates et al.* [1990b]; 9, *Andreae et al.* [1988b]; 10, *Berresheim* [1987]; 11, *Huebert et al.* [1993]; 12, *Andreae and Andreae* [1988a]; 13, *Andreae et al.* [1990]; 14, *Bingemer et al.* [1992]; 15, *Berresheim and Vulcan* [1992]; 16, *Quinn et al.* [1990].

mean observations averaged over several years. Given the large number of existing measurements, we do not attempt to give here an exhaustive inventory of the observations. Unless noted, the following tables (4 to 9) compare model results with observations performed during month or week campaigns. When provided by the authors, the median, mean, and range of observed values are reported. The model results are also compared to long-term observations (seasonal variations), when available.

5.1. DMS

As shown in Figure 4 which illustrates the model results (at the surface) for DMS in July, the calculated DMS concentrations are very low above most continental areas (less than 10 pptv), with somewhat larger values in tropical regions (about 25 pptv). They reach 300 pptv in the 0°-45° oceanic belt of the summer hemi-sphere. Due to the short lifetime of DMS (0.9 day as computed by the model), the distribution of this compound reflects mainly the source distribution.

A similar pattern appears in the DMS distribution simulated with the MOGUNTIA model [*Langner and Rodhe*, 1991]. The DMS concentrations calculated by IMAGES are however well below the values predicted by MOGUNTIA in the southern hemisphere around the Antarctic ocean, because our methodology to evaluate the emission fluxes differs from that of *Langner and Rodhe* [1991], who used measured seawater DMS concentrations and air-sea exchange rates. In that part of the world, the IMAGES results are nevertheless in good agrement with observations (within a factor 1.2, see Table 4 and Figure 4).

Few measurements have been conducted over continental polluted areas. Table 4 compares observed concentrations with model results. The typical ratio of
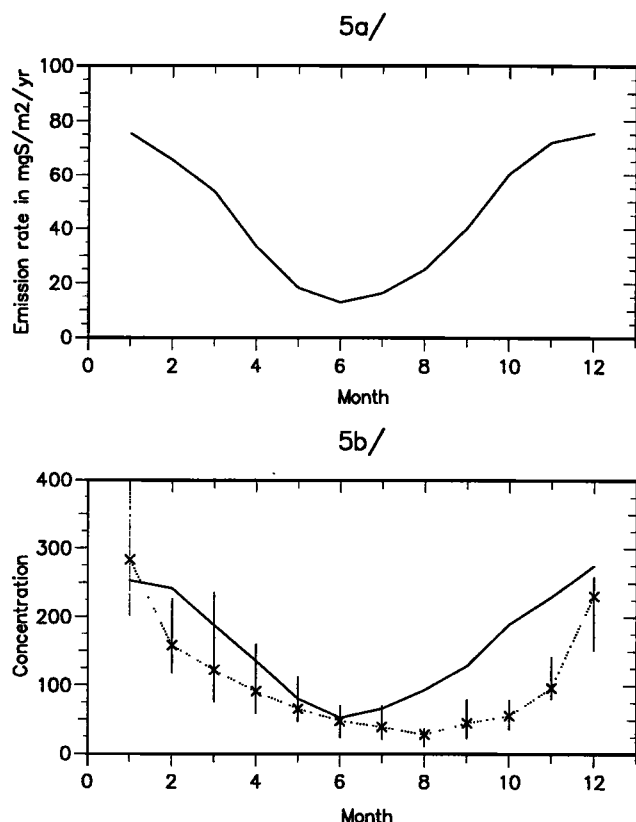
Figure 5. (a) DMS seasonal variation of emission fluxes at Amsterdam Island (37°50'S-77°30'E). Unit: mg S m^{-2} yr^{-1} . (b) DMS seasonal variation at Amsterdam Island (37°50'S-77°30'E). Concentrations are in parts per trillion by volume. Solid lines represent model calculations; connected symbols are measurements of *Nguyen et al.* [1990] and *Putaud et al.* [1992] averaged on 5 years of observations. Bars represent the lower and higher limits of observations.

mean observed to calculated DMS concentration ranges from 0.2 to 3. This agreement is relatively good given that the measured concentrations are highly variable in space and time and that our emission estimates are uncertain within a factor 2-3.

Figures 5a and 5b show the seasonal variation of DMS concentrations and emission fluxes at Amsterdam Island, in comparison with observations by *Putaud et al.* [1992]. Figure 6 compares the calculated DMS seasonal cycle with the *Ayers et al.* [1991] measurements. The observations were averaged over the available measurement periods (1984 and 1987-1990 for Amsterdam Island, and November 1988 to May 1990 for Cape Grim). At both stations, the calculated seasonal cycle is characterized by a maximum value in austral summer and a minimum in winter. However, the time when DMS concentrations begin to rise occurs somewhat too early in the model. This might be due to inaccuracies in our DMS emission fluxes. As suggested by Figures 5a-5b, the DMS seasonal variation at Amsterdam Island is driven by the seasonal cycle of the emissions. The modelled amplitude of the seasonal variation (ratio of
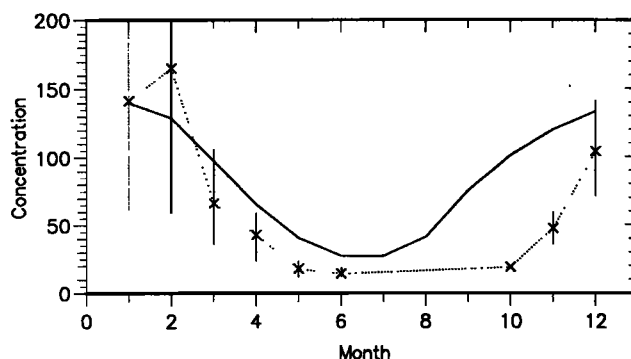
Figure 6. DMS seasonal variation at Cape Grim (40°41'S-144°41'E). Concentrations are in parts per trillion by volume. Solid lines represent model calculations; connected symbols are measurements of *Ayers et al.* [1991] averaged on the observations period (November 1988 to May 1990). Bars connect the lower and higher limits of observations.

maximum to minimum) is around 6 for the emission flux and 5.2 for the concentration. The latter ratio is at the lower boundary of the observed amplitude range (4.8 to 17).

5.2. DMSO

As a direct oxidation product of DMS by OH, DMSO is characterized by the same distribution pattern as that found for DMS (see Figure 7). However, the globally averaged lifetime of DMSO is shorter (4 hours), and its concentration is much lower than that of DMS. The predicted values are within the range of observations by *Harvey and Lang* [1986] (0.7-1.25 pptv) off the Florida coast in April (1.1 pptv). In remote parts of the tropical north Atlantic (around 10°N, 40°-60°W), DMSO modelled concentrations reach 3 pptv, which is slightly lower than the median value of approximately 5 pptv estimated by *Pzsenny et al.* [1990] during the WATOX (Western Atlantic Ocean Experiment) campaign in summer 1988. Because the available DMSO data are very limited, it is difficult to infer any conclusion from this comparison.

5.3. MSA

The production mechanism of MSA is poorly understood. As mentioned above, MSA is probably an ox-
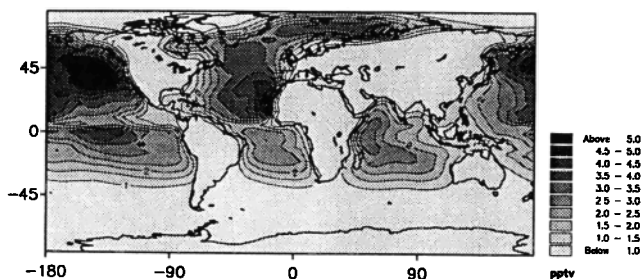
Figure 7. IMAGES DMSO distribution at the surface in July.

a/
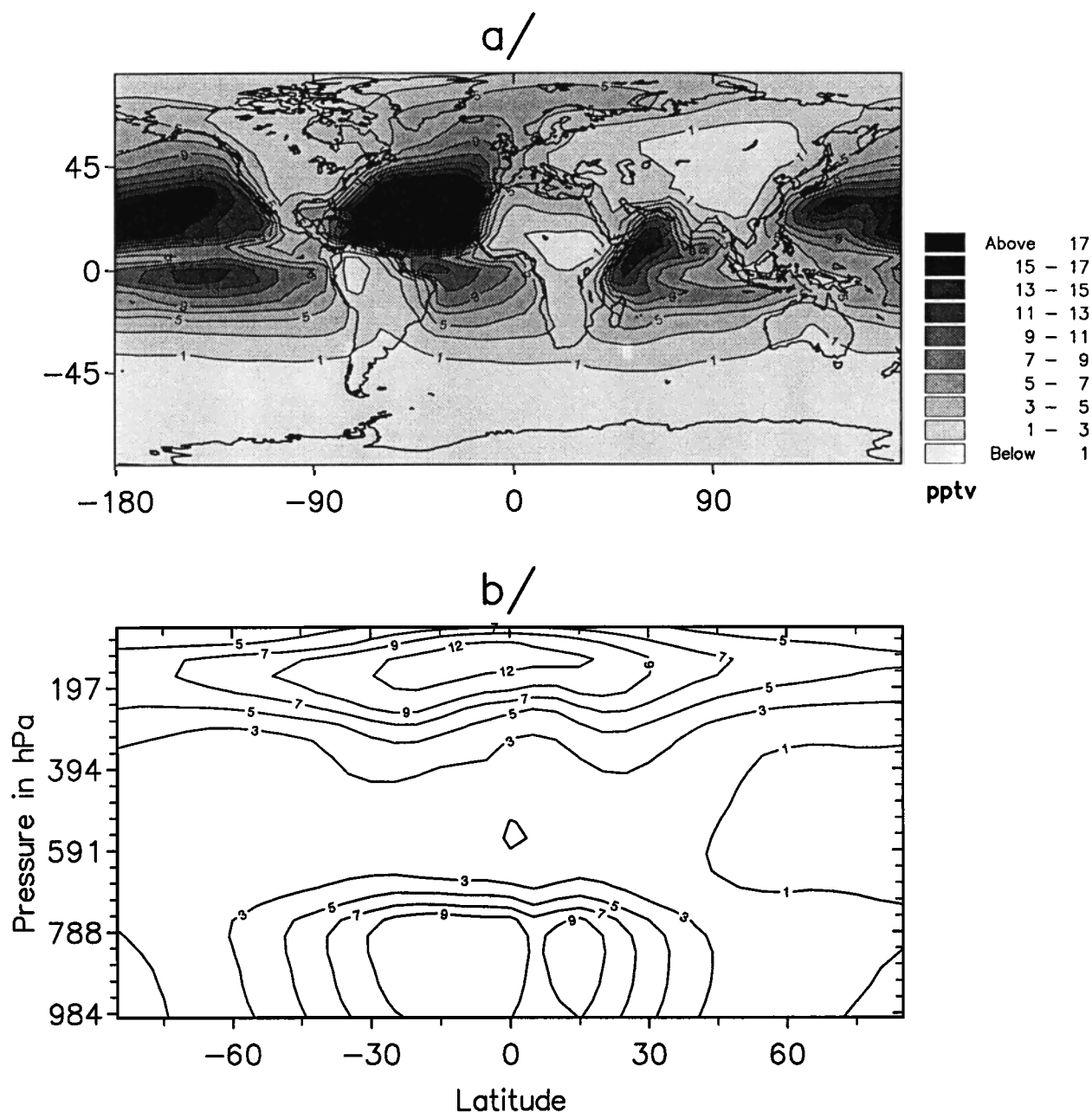
**Figure 8.** (a) IMAGES MSA distribution at the surface in July. (b) Zonal annually averaged MSA distribution (parts per trillion by volume).

idation product of DMS with OH, and is believed to be produced in large quantities when the abundance of nitrogen oxides is high [*Barnes et al.*, 1988]. We assumed that MSA was not produced by DMS+OH, but by DMSO+OH, following *Chatfield and Crutzen* [1990], whose reaction cycle reproduces well the tropical marine atmosphere. Figure 8a illustrates the MSA distribution in July, which is very similar to that of DMSO. Its longer global lifetime (6.1 days), however, allows this compound to be transported over larger distances, for example, over continental areas. Maximum values are above 20 pptv. (For MSA and nss-sulfates aerosols, 1 pptv represents 10^{-12} mole of the compound per mole of air in the same volume. The size distributions are

not considered for these particles in the calculations.) In the higher troposphere, where wet scavenging is less efficient and where MSA is transported by convective processes, MSA values reach 15 pptv in the equatorial belt (Figure 8b).

When compared to monthly averaged observations in remote marine areas, predicted MSA concentrations are within a factor 2-3 of observations in most cases (Figures 9a-9d). Nevertheless, the model underestimates MSA concentration by a factor of 2 to 5 above polluted areas (Figure 9d); this is probably due to simplifications in our chemical scheme, which are not relevant for such perturbed conditions, since we did not consider the influence of NO_x on MSA production.
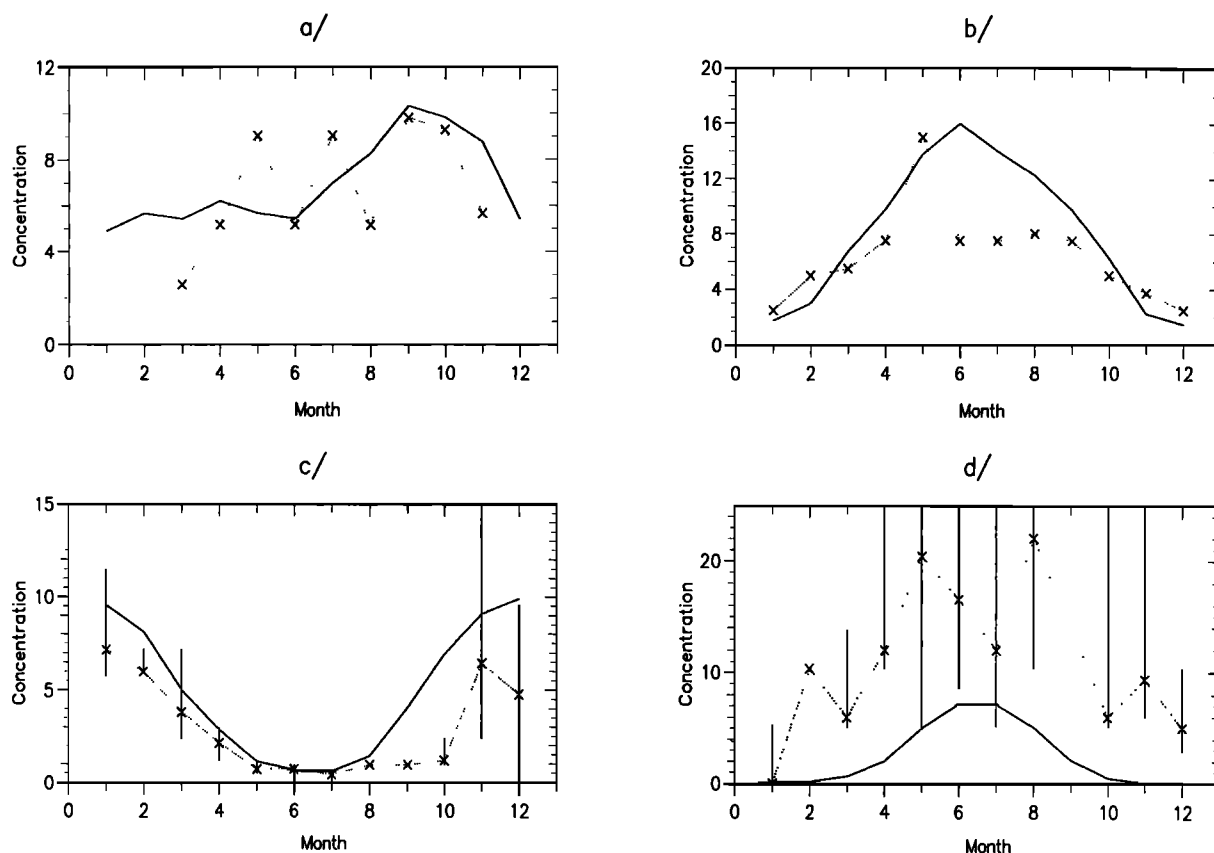
Figure 9. (a) MSA seasonal variation at Samoa (170°W-15°S). Concentrations are in parts per trillion by volume. Solid lines represent model calculations; connected symbols are observations of *Savoie and Prospero* [1989] (January 1981 to January 1982). (b) MSA seasonal variation at Midway (175°W-30°N). Concentrations are in pptv. Solid lines represent model calculations : connected symbols are observations of *Savoie and Prospero* [1989] (January 1981 to January 1982). (c) MSA seasonal variation at Cape Grim (40°41'S-144°41'E). Concentrations are in pptv. Solid lines represent model calculations; connected symbols are observations of *Ayers et al.* [1991] averaged on the measurements period (November 1988 to May 1990). Bars give the range of measurements. (d) MSA seasonal variation at Plymouth (50°10'N-4°8'W). Concentrations are in pptv.. Solid lines represent model calculations; connected symbols are observations of *Watts et al.* [1990] averaged on the measurements period (October 1985 to July 1987). Bars give the range of measurements.

5.4. H₂S

According to measurements by *Herrmann and Jaeschke* [1984] and *Saltzmann and Cooper* [1988], H₂S is present over oceans at concentrations around 20 pptv. However, to our knowledge, no H₂S concentration in marine waters has been reported, so that H₂S emissions from oceans were ignored in this model study. The existence of such an emission would, in fact, be in contradiction with the idea that an anoxic environment is necessary to produce H₂S [*Andreae*, 1985a]. However, as shown in Table 5, large discrepancies exist between observed and predicted concentrations over the oceans. Sensitivity studies show that an H₂S flux of 0.2 Tg S/yr is needed to explain the observed concentrations. The global lifetime of H₂S is calculated to be around 2.2 days. In the present version of the model, H₂S is mainly distributed over tropical forests which we consider to be its major source, with concentrations between 25 and 95 pptv (Figure 10a for January and Figure 10b for July).

As shown in Table 5, the model underestimates H₂S concentrations over tidal flats of northern Germany: the model grid cannot take into account the very localized, intensive H₂S emission fluxes from marshlands and tidal flats. Above tropical ecosystems, H₂S model concentrations are at the lower limit of the range of observations by *Delmas and Servant* [1983]. More recent measurements of emission fluxes by *Andreae and Andreae* [1988a] suggest however that H₂S released by soils is rapidly deposited under the tree canopy and that previous concentration measurements probably overestimated the concentrations above the tropical forests. This seems to be confirmed by the latest observations by *Andreae et al.* [1990] and *Bingemer et al.* [1992], who found much lower H₂S concentrations. Table 5 shows a very good agreement (less than a factor of 2) between these measurements and the model results.

A better estimate of H₂S sources seems necessary to simulate adequately the budget of this compound. It

Table 5. Measurements of H_2S at Several Locations at the Surface, Unless Noted, and Comparison With Calculated Concentrations for the Same Areas and Time Periods

Location	Time Period	Mean	Range	Model	Ref
Bahamas	June	59	10 - 260	0.4	1
Gulf of Mexico	September	46	30 - 90	3	1
Caribbean	Feb/March	8.5	0 - 20	5	1
Atlantic	October	28	10 - 100	3	2
Northern Germany	June/Oct		100 - 530	0.8	3
Tropics	January		15 - 6400	23	4
Amazon Basin	Dry season				5
- surface		30 ± 12		53	
Amazon Basin	Wet season				5
- mixed layer		47 ± 21		34	
- free troposphere		7 ± 7		8	
Congo	Feb/March				6
- surface - forest		42 ± 16		41	
- surface - clearing		24 ± 15		41	
- mixed layer		25 ± 16		29	
- free troposphere			7 - 13	5	

Concentrations are in parts per trillion by volume.
References: 1, *Saltzmann and Cooper* [1988]; 2, *Herrmann and Jaeschke* [1984]; 3, *Jaeschke et al.* [1980]; 4, *Delmas and Servant* [1983]; 5, *Andreae et al.* [1990]; 6, *Bingemer et al.* [1992].

appears, however, that H_2S has an insignificant impact on the global sulfur budget: it represents less than 0.2% of the total calculated sulfur mass and its oxidation accounts for less than 3% of the SO_2 production.

5.5. CS_2

CS_2 is mainly emitted by anthropogenic activities. Hence its modelled concentrations are highest over industrialized areas (from 20 to 150 pptv) and also downwind of the polluted regions due to its relatively long lifetime of 4 days (see Figures 11a and 11b). CS_2 is also present over oceans with concentrations of 5-25 pptv. These values are within the range of observations in the marine atmosphere, given in Table 6.

In the free troposphere, the model underestimates CS_2 concentrations by 1 to 2 orders of magnitude. In the boundary layer of the South Atlantic area, however, the recent measurements of *Bates et al.,* [1990a] suggest lower values than previously reported in other regions. The paucity of data on emission fluxes and concentrations makes it difficult to quantify the CS_2 cycle. This latter question seems however interesting to elucidate: if CS_2 does not contribute significantly to the sulfur budget (0.7% of the total calculated mass and 3% of SO_2 production), it can nevertheless play an important role as the only chemical precursor of COS.

5.6. SO_2

Due to the importance of the anthropogenic source of SO_2, its largest concentrations (a few parts per billion by volume) are predicted above the polluted areas of North America, Europe and the Far East (Figure 12). Smaller, but still large mixing ratios are also found over Africa and South America, mainly due to ore smelting operations. Above the oceans, SO_2 is mainly determined by its production following the oxidation of DMS

(80% of its total chemical production). Its concentrations range from 25 to 100 pptv (Figure 12).

Figures 13a and 13b display comparisons of the calculated surface mixing ratios of SO_2 with the measurements at numerous European sites reported by *EMEP* [*United Nations,* 1988]. Each point on the plots represents the modelled and observed values at one site (or several sites, when their geographical distance is less than 100 km), averaged over the winter months (October to March) or the summer months (April to September). Model values were interpolated from the nearest grid points. As can be seen on the figures, the spatial variability of SO_2 mixing ratio is high, due to the proximity of the emissions. A large part of the variability cannot be matched by the model, owing to its relatively coarse resolution. Both observations and model results show that the SO_2 abundance is lower in summer than in winter, due to its more efficient oxidation at that time. The modelled seasonal cycle is however too weak compared with the observations. The predicted concentrations are too high (by a factor of 2 on average) during summer, while in winter, the model compares relatively well with the observations. The mean winter concentration (averaged over all stations) is about 20% too high, and the ratio of observed to calculated concentrations ranges from 0.5 to 2.2. The observed values in 1983/1984 are generally lower than in 1979/1980, demonstrating the efficiency of sulfur emissions regulations.

The calculated SO_2 concentrations at other various sites are usually within the range of the observations at the surface, as shown in Table 7. The typical ratio between calculated and observed concentrations ranges from 0.2 to about 3. At 2 km altitude, the model tends to underestimate the observed concentrations. It is possible that in-cloud oxidation is too efficient in the model at low altitudes, or, since the model surface values are
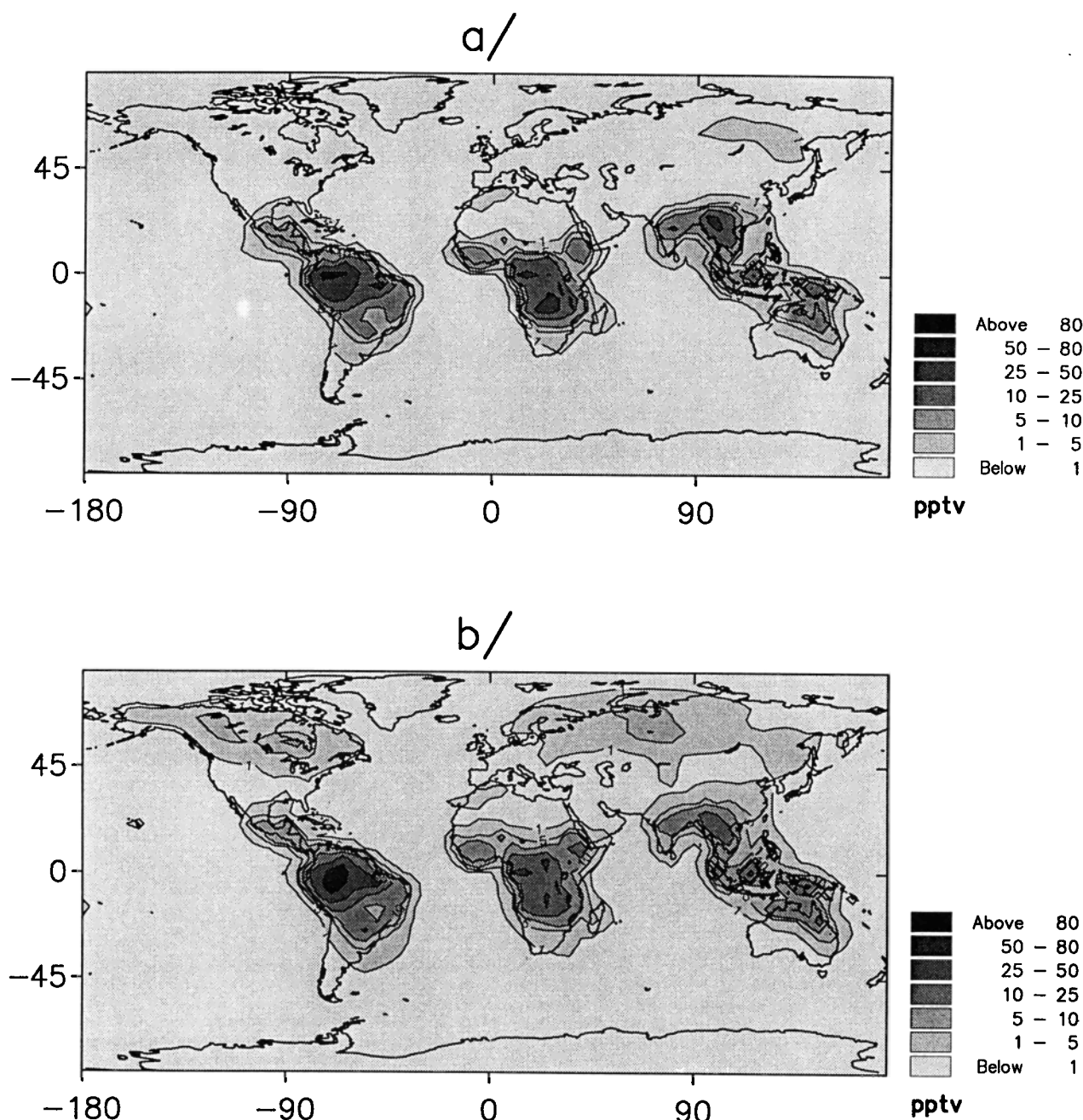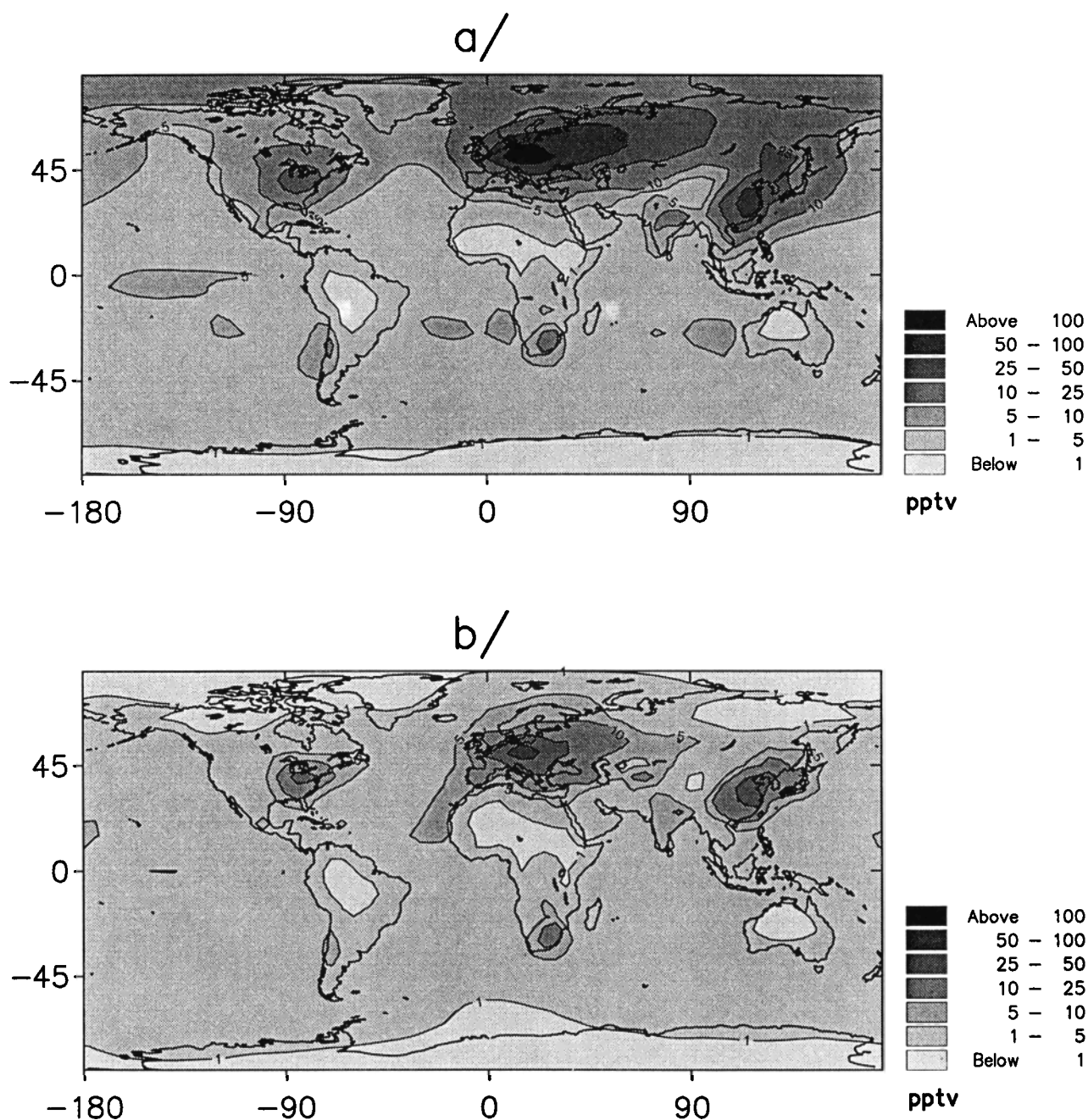
Figure 10. (a) IMAGES H$_2$S distribution at the surface in January. (b) IMAGES H$_2$S distribution at the surface in July.

generally not too low, that vertical mixing in the planetary boundary layer is too weak. At high altitudes (above 10 km), SO$_2$ concentrations are rather higher than the observed values by *Meixner* [1984]. Probable reasons for this are the volcanic source and the decoupling of wet scavenging and cloud convection in the model, as discussed in the following paragraphs for nss-sulfates.

Figures 14a and 14b illustrate the seasonal variations of SO$_2$ concentrations at a remote marine location and a polluted site, respectively. At Amsterdam Island, the DMS and SO$_2$ seasonal cycles have similar patterns, with a maximum in the austral summer and a minimum in winter. The predicted period of minimum concentration is however shorter than observed. The correlation between SO$_2$ and DMS reflects the fact that SO$_2$ is mainly determined by DMS oxidation in this area. In the Ohio River Valley, the model does not reproduce the observed seasonal cycle. As pointed out by *Langner and Rodhe* [1991], in-cloud chemistry should be treated with a better accuracy in polluted areas, in order to take into account winter oxidant limitation.

Figure 11. (a) IMAGES CS_2 distribution at the surface in January. (b) IMAGES CS_2 distribution at the surface in July.

5.7. Nss-sulfates

Nss-sulfates are mainly produced by in-cloud oxidation of SO_2, which represents around 90% of the SO_2 total chemical sink in the model. Because of the rapid conversion of SO_2 into sulfates, nss-sulfates concentrations are characterized by maxima of more than 1 ppbv over the regions where SO_2 is emitted, that is, industrialized areas (Figure 15a and 15b). The nss-sulfates lifetime of around 5 days, however, is longer than that of SO_2 (around 14 hours). This explains that relatively high concentrations of sulfate aerosol are found outside

the source regions. The calculated distribution of sulfates is broadly similar to that computed by *Langner and Rodhe* [1991]. In both models, concentrations are above 250 pptv over continental areas and reach maximum values of 2-3 ppbv over Europe and Asia in winter. In the subtropical belt, discrepancies between the two models arise, mostly from the way DMS emission fluxes have been estimated.

Figure 15c shows the annually and zonally averaged concentration of nss-sulfates as a function of latitude and altitude. Maximum values are located in the latitude belts of industrial activities and ore smelting

Table 6. Measurements of CS_2 at Several Locations at the Surface, Unless Noted, and Comparison With Calculated Concentrations for the Same Areas and Time Periods

Location	Time Period	Mean	Range	Model	Ref
North Atlantic	April/May	1.3	1.1 - 1.6	7	1
- open ocean	September	8.4	6.6 - 9.6	9.7	1
- coastal areas	April	13 ± 11	4.7 - 31	14	1
	August	37 ± 32	3.7 - 94	30	1
	September	11 ± 4.5	4.3 - 20	9	1
- estuaries	September	69 ± 63	7.2 - 184	21	1
West Atlantic	July/August	2.7 ± 2.5	1 - 11	5	2
Free Troposphere	July	115 ± 36 (6.1 km)		0.2 - 1	3
- 27-40°N		23 ± 7 (7.3 km)		0.2 - 1	3
- 68-74°W		26 ± 14 (7.3 - 7.9 km)		0.2 - 1	3
- South America	Annual mean	5.7 ± 1.9 (6 km)		0.1	4
- South Atlantic		≤2 (Boundary layer)		0.1	5
Georgia, U.S.A	July/Sep		<10 - 90	20	6

Concentrations are in parts per trillion by volume.
References: 1, *Kim and Andreae* [1987]; 2, *Cooper and Saltzmann* [1991]; 3, *Carroll* [1985]; 4, *Tucker et al.* [1985]; 5, *Bates et al.* [1990a]; 6, *Berresheim and Vulcan* [1992].

(around 45°N and 25°S). In the high troposphere, the predicted concentrations reach values up to 250 pptv, related to the relatively low efficiency of wet scavenging at these altitudes. These concentrations are 5 to 10 times higher than the values observed by *Lezberg et al.* [1979] around the tropopause. Section 5.8 shows that the high calculated concentrations are due to the explosive volcanic source (which releases sulphur at high altitudes), and to the decoupling of wet scavenging and convective mass transport in the model.

Table 8 and Figures 16a-16d compare calculated concentrations and observations at several sites. The broad features of the seasonal cycle of nss-sulfates are qualitatively accounted for by the model. The maximum seasonal differences are within a factor 3 of the range of observed values reproduced in Figures 16a, 16b, 16c, and 16d. At Mawson (61°E-68°S), the predicted amplitude of the seasonal cycle is smaller than observed,

probably reflecting a poor representation in the model of the Antarctic phytoplanctonic blooms.

As shown on Table 8 however, the model underestimates nss-sulfates at different remote sites in the Pacific Ocean. These discrepancies are dramatically reduced when the model is run with a lower deposition velocity for sulfates over oceans (0.05 cm/s), as described in section 5.8. The agreement between measurements and model results at the Pacific and Atlantic stations (Barbados, Oahu, Guam, Belau, Midway, Fanning, American Samoa, New Caledonia, and Norfolk Island) is then much closer, with ratios between calculated and observed values ranging from 0.48 to 1.18. At Fanning Island, discrepancies between measurements and calculated concentrations reach a factor of 6 in the high deposition velocity case and a factor of 2 in the low deposition velocity case. This might reflect the fact that Fanning Island is located in a highly productive equa-
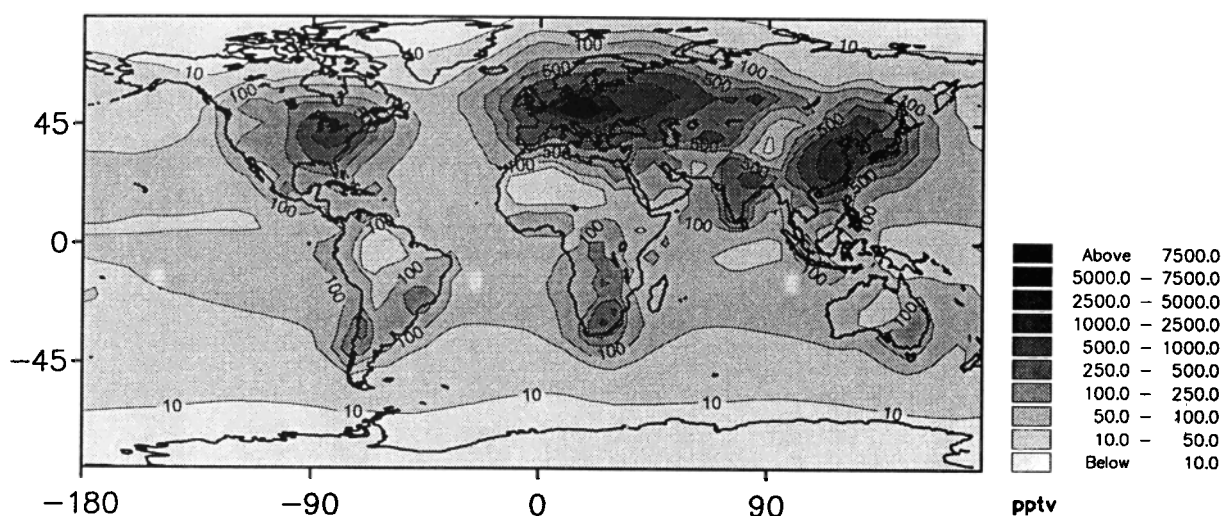
Figure 12. IMAGES annually averaged SO_2 distribution at the surface.
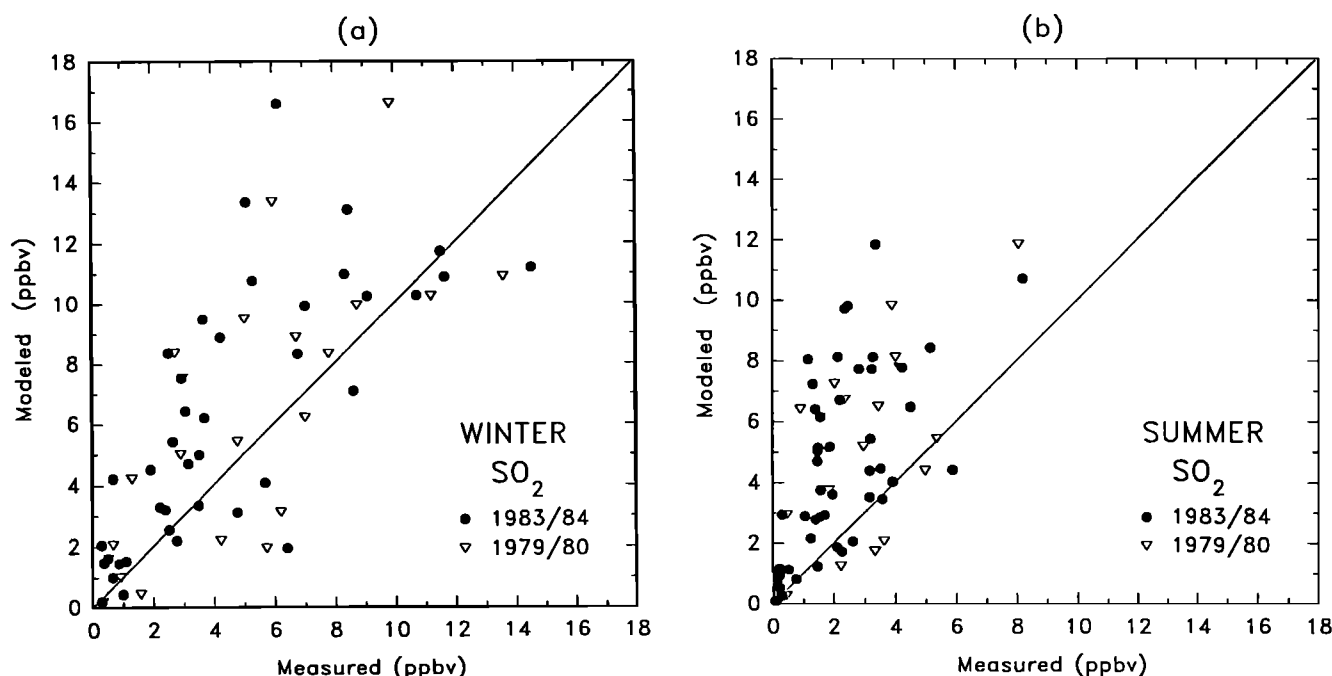
Figure 13. Calculated versus observed seasonal mean concentrations of SO_2 over Europe (a) in winter, and (b) in summer.

torial area, which is not represented in the model. At Midway, the model does not represent the nss-sulfate peak during late May/early June. According to the authors, these relatively high observed values might be related to transport of nss-sulfate associated with dust from Asia and Australia. In the low deposition velocity case, however, the seasonal cycle is not so well represented at the midlatitudes stations. This suggests the need for further improvements concerning both DMS emission fluxes and nss-sulfates deposition velocities.

Table 8 shows that the calculated concentrations at other polluted and nonpolluted sites are generally within the range of observations (ratio of mean observed to calculated concentration from 0.3 to 1.4). However, as shown by Figure 17a and 17b, the model underpredicts (by 35% on average) nss-sulfates concentrations at most European sites of the EMEP network in winter, while the calculated concentrations are slightly larger, on average, than the observations in summer (by 20%). As for SO_2, the seasonal cycle is not well represented by the model. The sensitivity test with lower deposition velocities described in section 5.8 produces better average values of calculated sulfates in winter. In this case, however, and consistently with the comparison for SO_2, the summer values calculated by the model are about 50% higher than in the observations. These results indicate the importance of better treating the spatial and temporal variations of dry deposition velocities in chemical models. The reasons for the summer overprediction are not clear, but should be related to dry/wet deposition of SO_2 (maybe too slow in the model in summer) and/or vertical mixing above the surface.

In the upper troposphere, the agreement is relatively good between calculated values and the observations by

Lazrus and Gandrud [1974] in the 12- to 14-km-altitude-range (Table 8).

The annually averaged value of the mass ratio MSA/SO_4^{2-} is calculated to be 0.5 and 0.13 at Mawson (68°S) and Samoa (14°S), respectively. These values are at the upper limit of the ratios measured by *Prospero et al.* [1991] (0.1-0.5) and *Saltzmann et al.* [1986] (0.044-0.103). According to *Berresheim* [1987], the difference between the two ranges of values may be explained by the lower temperatures at high latitudes, which favor MSA production by DMS+OH reaction via the addition pathway.

As can be seen in Table 9, the agreement is rather good (less than a factor of 2 in most areas) between the calculated annual wet deposition of nss-sulfates and measurements at several locations. The annual maximum of wet deposition is located around industrialized areas (Europe, Asia, and North America), with values reaching 2 g S m^{-2} yr^{-1}, as expected from the high sulfate concentration in these regions. In other parts of the world, the wet deposition is usually lower than 0.5 g S m^{-2} yr^{-1} (see Figure 18).

5.8. Sensitivity Studies

As mentioned before, and despite the modelling progress that has been made, many important processes determining the sulfur cycle are still poorly known, and are therefore crudely represented in the model. Several sensitivity studies were performed with the model in order to quantify the amplitude of the uncertainties related to some key parameters. Note that we did not intend to give here a systematic overview of the possible uncertainties in sulfur cycle modelling, which would be beyond the scope of this paper.

Table 7. Measurements of SO_2 at Several Locations at the Surface, Unless Noted, and Comparison With Calculated Concentrations for the Same Areas and Time Periods

Location	Time Period	Mean (Median)	Range	Model	Ref
NW. Atlantic	Summer				1
- remote		101	34 - 118	77	1
- coastal		156	26 - 640	500	1
- tropical		77	29 - 518	111	1
- 8-20°W, 30-45°N	July	78	26 - 181	186	2
- 30°W, 15-37°N	Annual mean	26	7 - 343	76	3
- 70°W, 40°N	Annual mean	1830		1974	4
- id., 2 km	Annual mean	140 (60)		30	4
Tropical Pacific					
- 145-165°W; 15°S-20°N	Feb/March	27	5 - 111	56	5
- 170°W; 10°S-15°N	April/May	30 ± 17	10 - 62	56	13
Tasmania	December	16	4 - 22	50	6
Amazon Basin	Dry season				7
- mixed layer		27 ± 10		43	
- free troposphere		18 ± 16		10	
Amazon Basin	Wet season				8
- mixed layer		24 ± 14		17	
- free troposphere		15 ± 8		3	
Georgia, U.S.A	July		3.6 - 4.1 ppbv	2.4	9
	August		0.1 - 1.3 ppbv	2.4	9
	September		0.1 - 5.6 ppbv	2.3	9
110°W, 0-70°N	Annual mean	89 ± 69		173	10
110°W, 0-57°S	Annual mean	57 ± 18		46	10
Central U.S.	Annual mean	690		657	11
- ~ 2.5 km	Annual mean	270		75	11
W. Europe					12
- 4 km	April	53 ± 18		38	12
- 7 km	April	21 ± 7		43	12
- 12.4 km	April	28 ± 4		78	12
- 8.5 km	September	85 ± 13		78	12
- 10.7 km	September	57 ± 14		134	12
- 13.2 km	September	25 ± 15		69	12
- 14.5 km	September	46 ± 13		69	12
- 3.4 km	May	93 ± 19		33	12
- 6.4 km	May	42 ± 10		50	12
- 10.7 km	May	41 ± 11		49	12
- 13.8 km	May	115 ± 22		93	12
- 10.7 km	December	10 ± 3		100	12
- 14.5 km	December	33 ± 9		77	12

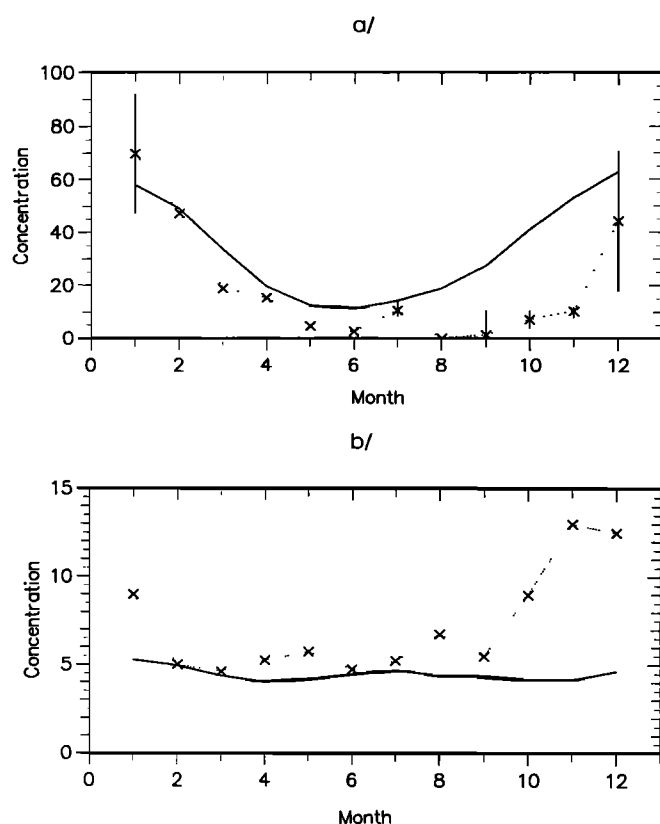Concentrations are in parts per trillion by volume.
References: 1, *Galloway et al.* [1990]; 2, *Herrmann and Jaeschke* [1984]; 3, *Nguyen et al.* [1983]; 4, *Thornton et al.* [1987]; 5, *Huebert et al.* [1993]; 6, *Berresheim et al.* [1990]; 7, *Andreae and Andreae* [1988a]; 8, *Andreae et al.* [1990]; 9, *Berresheim and Vulcan* [1992]; 10, *Maroulis et al.* [1980]; 11, *Boatman et al.* [1989]; 12, *Meizner* [1984]; 13, *Quinn et al.* [1990].

The results are summarized in Table 10, in terms of percentage differences (relative to the standard case discussed in the previous sections) for the globally integrated values of dry deposition, lifetime and burden of SO_2, and nss-sulfates. The table gives also the impact of the changes on the sulfate concentration in the mid-latitude high troposphere.

In the first test 1, cloud convection is assumed to be less efficient for water soluble species than for the other species, as suggested by *Costen et al.* [1988], to account for the fact that the soluble compounds are partly scavenged during convection, and therefore do not reach the high troposphere. A consequence of this treatment is that more of the compound is simply left in the boundary layer instead of being removed. However, as pointed out by *Costen et al.* [1988], the amount of such species left behind instead of being removed is small compared with the amount present in the boundary layer. The convection intensity (represented by the updraft densities, (19) in *Müller and Brasseur* [1994]) is reduced by a factor of 0.47 for SO_2 and DMSO and 0.35 for sulfates and MSA. Table 10 indicates that reduced convection has a more pronounced impact on sulfates than on SO_2. The sensitivity of the global budget of both species is found to be relatively small. Their burdens are slightly reduced (-7% for sulfates), because

a/

b/

Figure 14. (a) SO_2 seasonal variation at Amsterdam Island (37°50'S-77°30'E). Concentrations are in parts per trillion by volume. Solid lines represent model calculations; connected symbols are measurements of *Putaud et al.* [1992] averaged on 5 years of observations. Bars represent the lower and higher limits of observations. (b) SO_2 seasonal variation at Ohio River Valley (37°41'N-88°01'W). Concentrations are in parts per billion by volume; connected symbols are measurements of *Shaw and Paur* [1983] averaged on the observations period (May 1980 to August 1981).

nss-sulfates lifetimes are generally shorter in the lower troposphere than at higher altitudes. A large impact is predicted for nss-sulfates distribution in the higher troposphere: their concentrations at about 8.5 km in midlatitudes are found to be reduced by about 36%.

In our second sensitivity test, we suppressed the high altitude injection of SO_2 associated with explosive volcanism. Being aware of the fact that our volcanic source in IMAGES is climatological and ignores the extremely episodic character of eruptive volcanism, this test allows us to estimate a possible "background" distribution of sulfur species in the absence of any large VEI eruptions. The results (case 2 in Table 10) show a reduction in the SO_2 global amount of almost 30%, larger than would be expected from the reduction of the global SO_2 source (-7 Tg S/yr). This is due to the longer lifetime of SO_2 at the high altitudes where sulfur is released by explosive volcanoes. An important reduction of midlatitude high tropospheric sulfates concentrations is also predicted (-24%). Thus it appears that our high-sulfate

concentrations at these altitudes (compared with observations) could be explained partly by (1) the decoupling of wet scavenging and convective mass transport and (2) partly by the explosive volcanic source. Taking into account the new assumptions, the midlatitude sulfates concentrations would reach 120 pptv in the higher troposphere, which is at the upper limit of observations by *Lezberg et al.* [1979] over the United States.
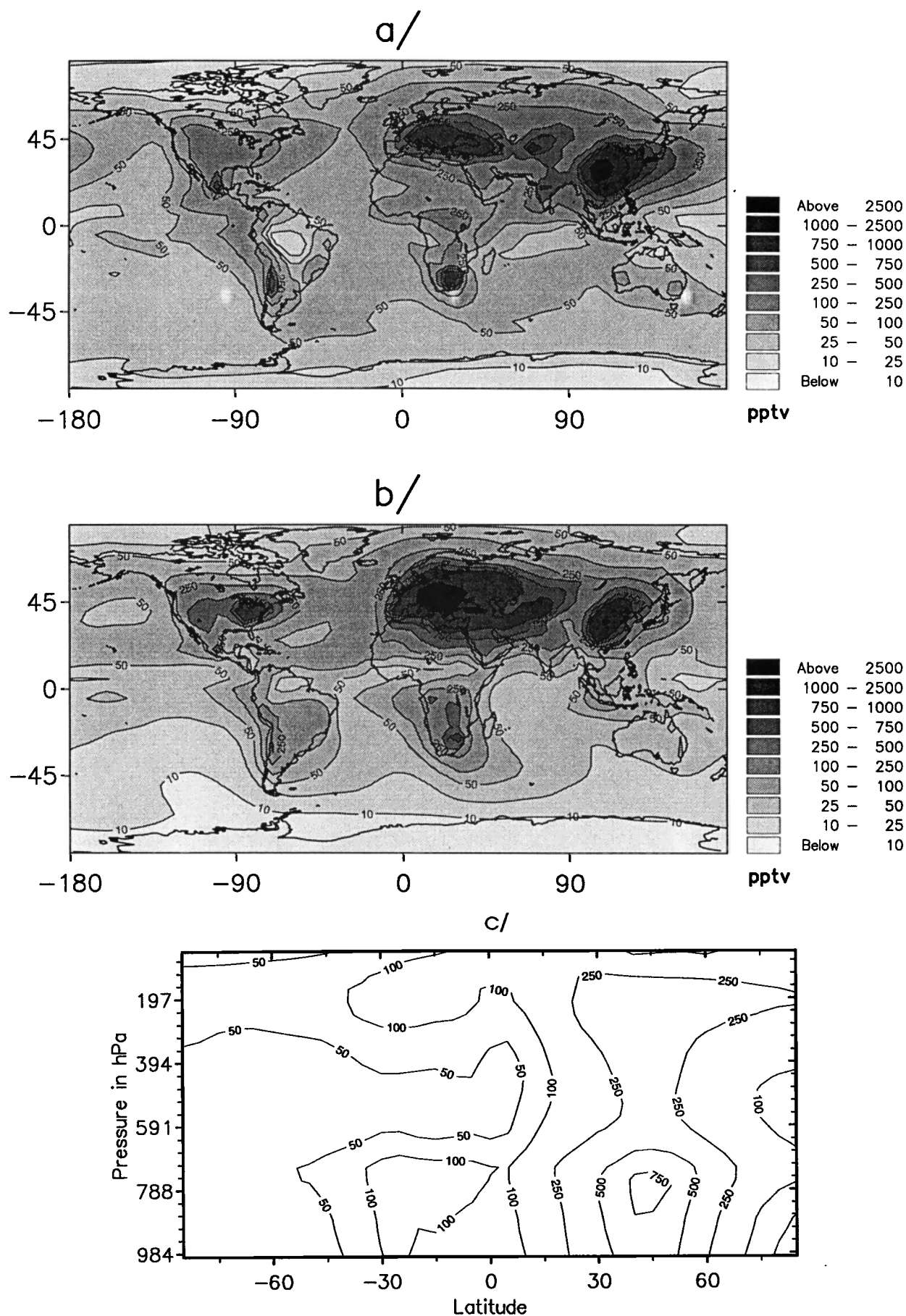
The SO_2 deposition velocities adopted in the IMAGES model are in the range of observed values (0.16-4 cms^{-1} over water and 0.1-2.5 cms^{-1} over land [*Voldner et al.*, 1986]). The measured velocities are however highly variable, depending on location, meteorological conditions, and time of the day. Our test case 3 shows that reducing SO_2 dry deposition velocity by a uniform factor of 1.5 increases the SO_2 burden by 10%. It also increases nss-sulfates burden by 13%, as more SO_2 is converted into sulfates. In this case, total dry deposition accounts for 75% of SO_2 total deposition. The increase of SO_2 conversion into sulfates explains the slight reduction of SO_2 chemical lifetime (defined as the ratio of the total mass burden to the chemical sink).

Finally, Table 10 shows results for the test case 4 where the sulfates deposition velocity is reduced to 0.25 cm/s over land and 0.05 cm/s over ocean, closer to the values given by *Walcek et al.* [1986]. This reduction has a large impact on the sulfates burden, which increases by 28.5%. It also induces an increase in high tropospheric sulfate concentrations. The importance of these numbers show that further efforts must be undertaken to refine the estimates of SO_2 and sulfate deposition velocities.

6. Global Budgets

Figure 19 schematically illustrates the global sulfur budget computed by the IMAGES model. Tables 11, 12, and 13 provide for each compound, the global turn-over time and the different productions and sinks terms (the turn-over time is computed as the ratio of the total mass burden to the total sink, with dry and wet deposition included).

The global DMS turn-over time is estimated to be 0.9 day. This value is lower than the estimate of 3 days by *Langner and Rodhe* [1991]. The reasons for this discrepancy are unclear. The kinetic rate constants used for the reaction of DMS with OH are identical in both studies. Part of the difference might be due to the differences in the OH fields, and to the fact that the reaction of DMS with NO_3 (which contributes to about 20% of the total sink of DMS in our calculations) has been neglected by *Langner and Rodhe* [1991]. Also, the higher emission fluxes used by the latter study in the high southern latitudes tend to increase the global lifetime of DMS, due to the low OH abundance in these regions. Our lower turn-over time results also in a lower global burden for DMS (0.05 Tg S) compared with the value estimated by *Langner and Rodhe* (0.22 Tg S), since the DMS source strength is similar in both studies (20 and 16 Tg S/yr).

Figure 15. IMAGES sulfates distribution at the surface in (a) January, and in (b) July. (c) Zonal annually averaged sulfates distribution (parts per trillion by volume).

Table 8. Measurements of NSS-Sulfates at Several Locations at the Surface, Unless Noted, and Comparison With Calculated Concentrations for the Same Areas and Time Periods

Location	Time Period	Mean	Range	Model	Ref
NW. Atlantic	Summer				1
- 25-40°W; 55-65°N		157	35 - 903	98	
- 40-50°W; 45-55°N		14	1.4 - 46 5	118	
- 55-75°W; 35-40°N		299	48 - 4956	410	
- 60-70°W; 30-35°N		265	96 - 549	101	
Barbados	Annual mean	192 ± 53		88	2
NE. Pacific	May				3
- 0 km			40 - 150	131	
- 1 km			25 - 100	181	
- 2 km			50 - 120	133	
- 3 km			75 - 150	127	
Pacific	Annual mean				4
- Oahu		127 ± 15		56	
- Guam		128.5 ± 51		73	
- Belau		155 ± 26		72	
- Midway		166 ± 196		76	
- Fanning		163 ± 46		24	
- Samoa		101 ± 41		45	
- New. Cal.		128 ± 100		46	
- Norfolk		82 ± 37		40	
Tropical Pacific					
- 145-165°W; 15°S-20°N	Feb/March	124	50 - 173	37	5
- 170°W; 10°S-15°N	April/May	99 ± 52	45 - 213	35	11
Amazon Basin	Dry season				6
- surface		118 ± 119		68	
- mixed layer		129 ± 50		84	
- free troposphere		16 ± 7		59	
Amazon Basin	Wet season				7
- surface		67 ± -		27	
- mixed layer		76 ± 56		32	
- free troposphere		11 ± 4		20	
Georgia, U.S.A	Jul-Sep		1.5 - 6.8 (ppbv)	1.1	8
(Sub-) Arctic	Annual mean				9
- 79°N-12°E		167		81	
- 75°N-19°E		219		156	
- 70°N-25°E		368		320	
Tropopause	Spring				10
-75°N-51°S-~ 90°W	12-14 km	27 - 310		79 - 180	

Concentrations are in parts per trillion by volume.
References: 1, *Galloway et al.* [1990]; 2, *Savoie et al.* [1989]; 3, *Andreae et al.* [1988b]; 4, *Savoie and Prospero* [1989]; 5, *Huebert et al.* [1993]; 6, *Andreae and Andreae* [1988a]; 7, *Andreae et al.* [1990]; 8, *Berresheim and Vulcan* [1992]; 9, *Heintzenberg and Larssen* [1983]; 10, *Lazrus and Gandrud* [1974]; 11, *Quinn et al.* [1990].

The total H_2S mass is also lower than suggested in one-dimensional studies of the remote troposphere by *Toon et al.* [1987] and *Sze and Ko* [1980], since these models used a source flux of 1-5 Tg S/yr and 10 Tg S/yr, respectively, compared to our global source strength of 0.5 Tg S/yr. H_2S estimated turn-over time is 2.2 days, which is within the range of the lifetimes estimated by these authors.

The total CS_2 mass is estimated to be equal to 5.10^{-3} Tg S and the turn-over time to 4 days. Uncertainties on CS_2 fluxes and concentrations in the free troposphere are reflected in the large range of total burdens and turn-over times estimated by previous studies. According to *Toon et al.* [1987], CS_2 total burden is 0.07 Tg S with a global source strength of 5 Tg S/yr and a life-

time of 6 days. Using a source strength 10 times higher, *Sze and Ko* [1980] estimate a total burden of 0.6 Tg S. The rate constant they used however is 10 times lower than in our study and corresponds to a lifetime of 45 days. These modelling studies are to our knowledge, the most recent in reporting CS_2 concentrations. However, taking into account the different emission fluxes and chemical rates they used, it is difficult to infer any conclusion from this comparison.

DMSO is also present in very low global quantity in the atmosphere (2.10^{-3} Tg S) and its turn-over time is very short (around 4 hours). Its major sink results from the destruction by OH. Dry deposition accounts for 60% of the DMSO total deposition.

In contrast, the MSA turn-over time is relatively long
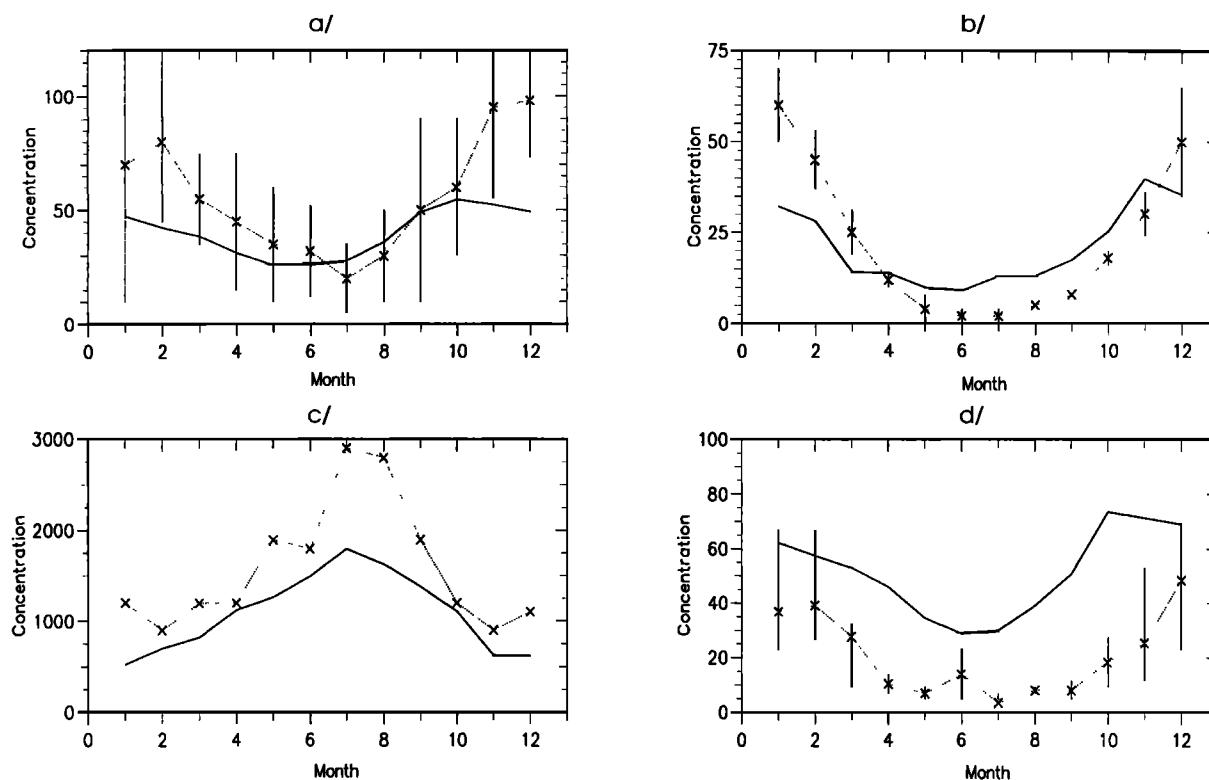
Figure 16. (a) Sulfates seasonal variation at Norfolk (168°E-30°S). Solid lines represent model calculations; connected symbols are measurements of *Savoie and Prospero* [1989] averaged on 5 years of observations. Bars connect the lower and higher limits of observations. (b) Sulfates seasonal variation at Mawson (61°E-68°S); connected symbols are measurements of *Prospero et al.* [1991] averaged on the observations period February 1987 to October 1989. Bars connect the lower and higher limits of observations. (c) Sulfates seasonal variation at Ohio River Valley (37°41'N-88°01'W); connected symbols are measurements of *Shaw and Paur* [1983] averaged on the observations period (May 1980 to August 1981). (d) Sulfates seasonal variation at Cape Grim (40°41'S-144°41'E); connected symbols are observations of *Ayers et al.* [1991] averaged on the measurements period (November 1988 to May 1990). Bars give the range of measurements. All concentrations are given in parts per trillion by volume.
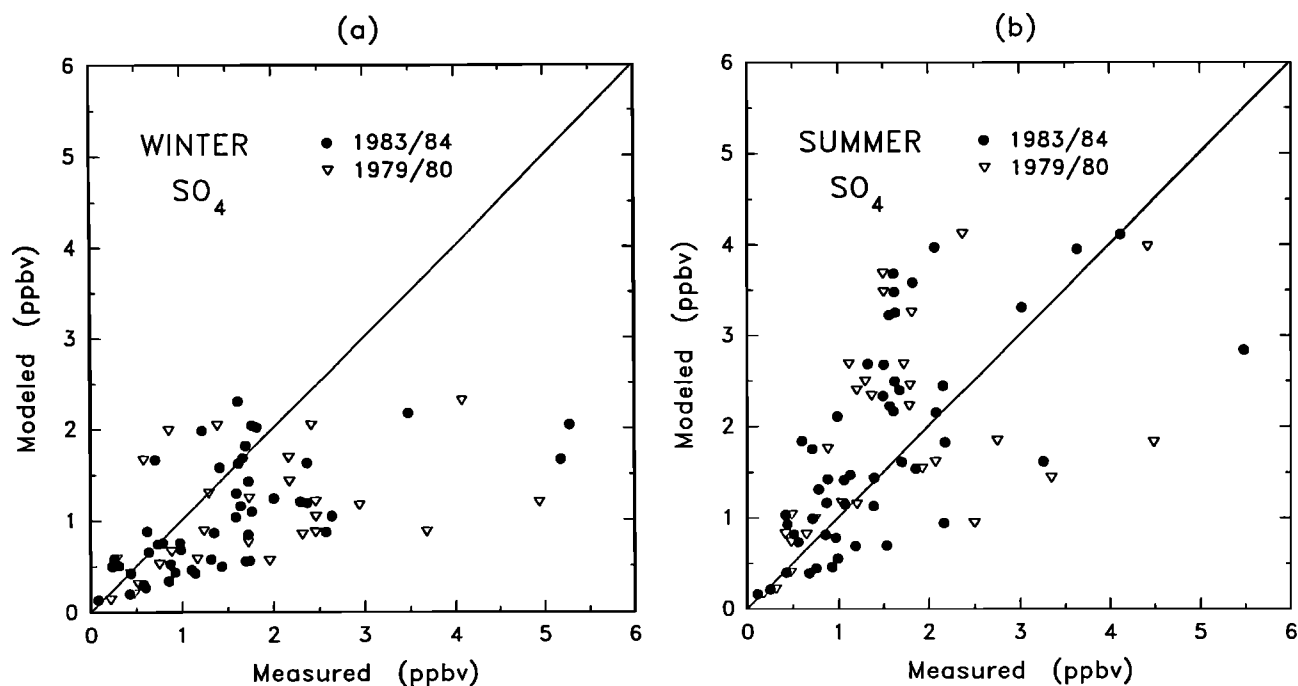
Figure 17. Calculated versus observed seasonal mean concentrations of nss-sulfates over Europe, (a) in winter and (b) in summer.

Table 9. Measurements of Sulfate Wet Deposition at Several Locations and Comparison With Calculated Values for the Same Areas and Time Periods

| Location	Measurements	Model	Ref
Eastern U.S. (maximum)	1300	1055	1
Western U.S. (maximum)	270	375	2
Europe (maximum)	2000	2120	3
East Africa	150	139	4
San Carlos, Venezuela	170	153	5
Poker Flat, Alaska	32	57	5
Lake Calado, Brazil	120	157	6
Australia	64	62	7
Antarctic	0.8 - 1.3	1.3 - 3.7	8
Atlantic			
- 0-30°N	200 - 300	50 - 500	9
- Bermuda	450	481	5
- South Atlantic	50 - 100	1 - 200	9
Pacific			
- Samoa	66	351	10
- New Zealand	67	155	6
- Central Tasmania Sea	130	94	6
Amsterdam Island	100	143	11

Measurements are in milligrams sulfur per square meter per year.
References: 1, *Barrie and Hales* [1984]; 2, *Georgii* [1982]; 3, *EMEP* [1984]; 4, *Rodhe et al.* [1981]; 5, *Galloway et al.* [1982]; 6, *Galloway* [1985]; 7, *Likens et al.* [1987]; 8, *Legrand and Delmas* [1984]; 9, *Varhelyi and Gravenhorst* [1983] (in this case, only ranges of values are given); 10, *Pzsenny et al.* [1982]; 11, *Galloway and Gaudry* [1984].

(6.1 days) and corresponds approximately to the lifetime of aerosols in the atmosphere, as inferred from measurements of radioactive species [*Junge*, 1963]. Wet scavenging is the major sink for MSA (58%) which is only produced by the reaction of DMS with OH.

The turn-over time of SO_2 is found to be 0.6 days, or about half the value estimated by *Langner and Rodhe* [1991]. It is, however, similar to the lower tropospheric lifetime estimated by *Lelieveld* [1990] using a cloud chemistry box model applied for several altitudes and latitudes. As derived from Table 12, the average contributions to the global SO_2 tropospheric sink are 45.1%

for dry deposition, 4.1% for wet deposition, 5.3% for gas phase oxidation and 45.5% for aqueous phase oxidation. These values are close to the range of estimates by *Rodhe and Isaksen* [1980] (with a global two-dimensional model) and by *Langner and Rodhe* [1991]. The *Rodhe and Isaksen* [1980] and *Langner and Rodhe* [1991] estimates are, respectively, 49.5-32.3% for dry deposition, 7.5-15% for wet scavenging, 16.5-8.3% for OH oxidation, and 20.5%-44.4% for aqueous SO_2 conversion. Dry deposition accounts for 90% of total deposition of SO_2 (60 Tg S/yr). This corresponds to almost twice the amount estimated by *Langner and Rodhe*
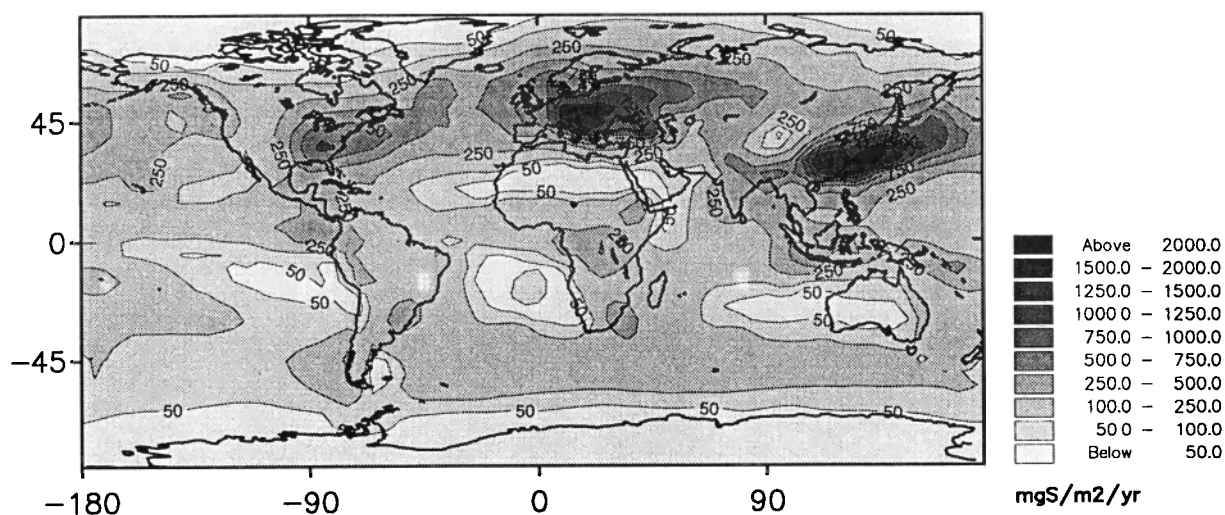
Figure 18. IMAGES annually averaged sulfate wet deposition.

Table 10. Sensitivity of SO_2 and NSS-Sulfates Budgets (Global Chemical Lifetime, Globally Integrated Dry Deposition and Global Burden) and High Tropospheric NSS-Sulfates Concentrations at Midlatitudes, to Changes in Dry Deposition Velocities, Convective Transport Parameterization and the Volcano Source

	Standard Case Values	Reduced Convection, 1	No Explosive Volcanism, 2	Reduced vd_{SO_2}, 3	Reduced vd_{SO_4}, 4
SO_2					
Chemical lifetime	1 day	+ 0.9	- 18.8	- 3.4	
Dry deposition	55 Tg S/yr	+ 3.2	+ 0.6	- 18.3	
Burden	0.2 Tg S	- 1.1	- 26.6	+ 10.0	
Nss-sulfates					
Turn-over time	4.7 days	+ 0.6	- 0.3	+ 0.4	+ 7.7
Dry deposition	17 Tg S/yr	+ 10.4	+ 0.0	+ 17.2	- 39.4
Burden	0.8 Tg S	- 7.1	- 13.6	+ 12.8	+ 28.5
Concentration at midlatitude, z =8.5 km	200 pptv	- 36.4	- 23.5	+ 13.5	+ 16.1

In the case of nss-sulfates, the global turn-over time is considered. See text for further details.

[1991] (30.5 Tg S/yr) because of the higher deposition velocities used in our work. This value is 1.1 times higher than the quantity derived from *Warneck* [1987] on the basis of emission estimates and flux considerations. The SO_2 burden (0.2 Tg S) is close to the estimated value of 0.34 Tg S by *Langner and Rodhe*, [1991]. As shown in Table 12, in-cloud conversion of SO_2 into sulfates accounts for 90% of SO_2 total chemical sinks. This value is larger than that of *Langner and Rodhe* [1991] (84%), in spite of the similar approaches, probably because of the different cloud data used. It is in good agreement with *Lelieveld* [1990] calculations (90-95%).

The turn-over time for nss-sulfates is 4.7 days, which is similar to the estimate by *Langner and Rodhe* [1991]. The major sink for sulfates is wet deposition, with 73% of the total sink. This value is close to the estimate by *Rodhe and Isaksen* [1980] (75%). The higher deposition velocities used for nss-sulfates in the IMAGES model result again in a lower contribution for wet scavenging to sulfate total sink, compared to the estimate

of 84% by *Langner and Rodhe* [1991]. In terms of absolute quantities, our estimate for wet scavenging is 44.7 Tg S/yr and it compares well with the value calculated by these authors (44.5 Tg S/yr). It is also close to the estimate derived from measurements in Germany by *Georgii* [1982] (45 Tg S/yr).

7. Discussion and Conclusion

As shown in the previous sections, the concentrations of sulfur compounds are mainly controlled by SO_2 anthropogenic sources (industrial activities and biomass burning) which maintain values larger than 1 ppbv SO_2 above continental areas, and by the oceanic sources of DMS, which contribute to 300 pptv in some oceanic regions.

Comparisons between observed and predicted concentrations are difficult to perform, since there is no observation of tropospheric sulfur gases on the global scale. One ought to be cautious when comparing calculated abundances with measured concentrations at lo-
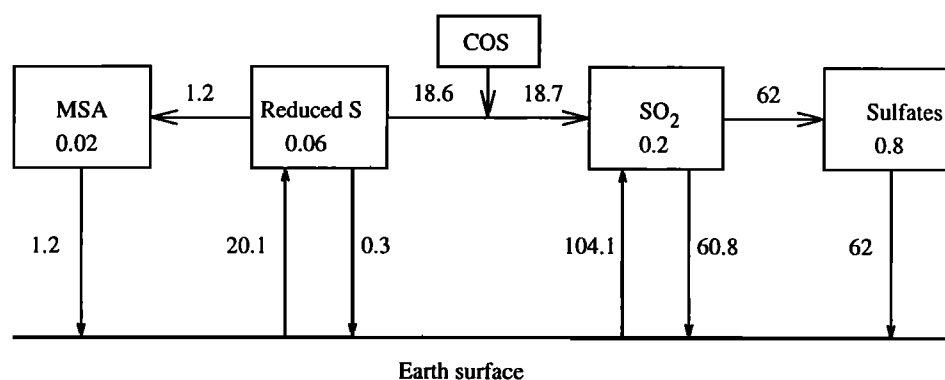
Figure 19. Schematic diagram of the atmospheric sulfur cycle developed in the model IMAGES. Reduced sulfur compounds include DMS, H_2S, CS_2 and DMSO. Burdens are indicated in teragrams sulfur. Arrows represent emission and deposition fluxes, and conversion into other compounds, and are expressed in teragrams sulfur per year.

Table 11. Annual Sulfur Budget in Tg S /yr (Flux, Sinks and Productions), in Tg S (Burden) and in Days (Turn-Over Time)

	DMS	CS_2	H_2S	DMSO	MSA	SO_2	sulfates
Burden	0.05	0.005	0.003	0.002	0.02	0.2	0.8
Turn-over time	0.9	4	2.2	0.18	6.1	0.6	4.7
Production terms	19.5	0.5	0.5	4.0	1.2	122.8	62
Chemical source	0	0	0	4.0	1.2	18.7	62
Emission	19.5	0.5	0.5	0	0	104.1	0
Sink terms	19.5	0.5	0.5	4.0	1.2	122.8	62
Chemical sink	19.5	0.5	0.5	3.5	0	62.8	0
Deposition	0	0	0	0.5	1.2	60	62

cal sites during a short period, as the predicted values are averages on a $5°$ x $5°$ grid and are representative of a climatological situation. Long-term measurements at remote sites are better suited for comparison with our results. Comparisons of observed and calculated seasonal cycles at pristine sites generally show a good agreement, within a factor of 2-3 at worst. The performance of the model is similar in polluted areas of Europe and North America, where a large number of measurements has been reported for SO_2 and sulfates. Nevertheless, the model suffers from many uncertainties caused by the simplifying assumptions which were adopted. These uncertainties are as follows:

1. Observed H_2S concentrations are systematically underestimated by the model, unless we add a H_2S emission flux of 0.2 Tg S/yr by the oceans. Field measurements of oceanic H_2S are necessary to better simulate the H_2S seasonal cycle.

2. DMS emissions and concentrations are estimated within a factor of 2-3 and should be improved by investigating the link between DMS emission fluxes and available biological data.

3. Predicted CS_2 concentrations in the free troposphere are also lower than observations. It is not currently possible to determine if the reported concentrations are too high or if the flux estimates for the open ocean are too low.

4. We did not take into account the nighttime production of MSA by DMS in presence of NO_3. This may explain the low MSA concentrations predicted in polluted areas. Further kinetic studies are needed to investigate the oxidation pathways of DMS and its reaction products.

5. SO_2 and nss-sulfates deposition velocities are, though within the range of previous estimates, somewhat higher than values used in several other regional or global modelling studies. Sensitivity studies have shown that using reduced deposition velocities may im-

Table 12. As Table 11 for SO_2

	SO_2	
	Total	Fraction
Burden	0.2	
Turn-over time	0.6	
Production terms	122.8	
Chemical production	18.7	
H_2S oxidation	0.6	3%
COS oxidation	0.1	0.5%
DMS oxidation	15.1	81%
CS_2 oxidation	0.55	3%
DMSO oxidation	2.35	12.5%
Emissions	104.1	
Sink Terms	122.8	
Chemical sinks	62	
Gas-phase oxidation	6.5	10%
In-cloud oxidation	55.5	90%
Wet scavenging	5	
Stratospheric sink	0.8	
Dry deposition	55	

Table 13. As Table 11 for NSS-Sulfates

| | Nss-Sulfates | |
	Total	Fraction
Burden	0.8	
Turn-over time	4.7	
Production terms	62	
Chemical production	62	
SO$_2$ gas-phase oxidation	6.5	10%
In-cloud SO$_2$ oxidation	55.5	90%
Sink Terms	62	
Wet scavenging	45	73%
Dry deposition	17	27%

prove the model results in terms of annual averages but not in terms of seasonal variations. Further effort is needed to address this question.

6. The volcanic source has to be improved since it is assumed to produce SO$_2$ continuously in the troposphere. It is one reason for the overestimation of modelled nss-sulfates in the high troposphere.

7. The major uncertainties in the simulated sulfur cycle arise from the parameterization of aqueous chemistry and wet scavenging, in relation with convective transport. Although the predicted wet deposition of sulfates is in good agreement with some measurements, further comparison with observed vertical profiles is necessary to check the consistency of the wet scavenging parameterization. In this respect, the decoupling of wet scavenging and convective mass transport is one of the model limitation and has been proved to partly induce a overestimation of nss-sulfates in the upper troposphere. In-cloud SO$_2$ chemistry has also to be refined since comparison with the few measurements at 2 km suggests that the model underestimates SO$_2$ concentrations.

Despite these deficiencies and taking into account the few measurements of sulfur compounds in the free troposphere, the model provides a reasonably consistent picture of the global sulfur cycle, with a better resolution and a more detailed chemistry cycle than in previous global model studies. Efforts should be undertaken to narrow the uncertainties, for example, by further confronting the model calculations with the observations. In this respect, long-term ("climatological") measurements at remote sites are best suited to validate the model. Measurements of sulfur species in the free troposphere and near the tropopause are clearly needed. Field campaigns are also necessary to understand the different components of the sulfur cycle, for example, in terms of aqueous chemistry and wet scavenging; but the resulting measurements are more difficult to interpret, as they are subject to important fluctuations due to local meteorological conditions and are affected by the variability of the emissions. Following the validation process, the next step will be to use the model to

help understand the role of the sulfur cycle in climate and global changes. Previous studies demonstrated the importance of sulfates in the Earth's radiation budget. Sulfur species are also believed to affect the budget of other tropospheric compounds (nitrogen oxides, OH, ...) through heterogeneous reactions on sulfate aerosols [*Dentener and Crutzen*, 1993].

References

Andreae, M. O., and H. Raemdonck, Dimethyl sulfide in the surface ocean and the marine atmosphere: A global view, *Science*, *221*, 744-747, 1983.

Andreae, M. O., The emission of sulfur in the remote atmosphere (background paper), in *The Biogeochemical Cycling of Sulfur and Nitrogen in the Remote Atmosphere*, edited by J. N. Galloway, R. J. Charlson, M. O. Andreae and H. Rodhe, pp. 5-26, D. Reidel, Norwell, Mass., 1985a.

Andreae, M. O., R. J. Ferek, F. Bermond, K. P. Byrd, R. T. Engstrom, S. Hardin, P. D. Houmere, F. LeMarrec, H. Raemdonck, and R. B. Chatfield, Dimethyl sulfide in the marine atmosphere, *J. Geophys. Res.*, *90*, 12,891-12,900, 1985b.

Andreae, M. O., The ocean as source of atmospheric sulfur compounds, in *The Role of Air-Sea exchange in Geochemical Cycling*, edited by P. Buat-Ménard, pp. 331-362, D. Reidel, Norwell, Mass., 1986.

Andreae, M. O., and T. W. Andreae, The cycle of biogenic sulfur compounds over the Amazon basin, 1, Dry Season, *J. Geophys. Res.*, *93*, 1487-1497, 1988a.

Andreae, M. O., H. Berresheim, T. W. Andreae, M. A. Kritz, T. S. Bates, and J. T. Merrill, Vertical distribution of dimethylsulfide, sulfur dioxide, formic acid, aerosol ions, and radon over the Northeast Pacific Ocean, *J. Atmos. Chem.*, *6*, 149-173, 1988b.

Andreae, M. O., H. Berresheim, H. Bingemer, D. J. Jacob, B. L. Lewis, S.-M. Li, and R. W. Talbot, The atmospheric sulfur cycle over the Amazon basin, 2, Wet Season, *J. Geophys. Res.*, *95*, 16,813-16,824, 1990.

Andreae, M. O., and R. J. Ferek, Photochemical production of carbonyl sulfide in seawater and its emission to the atmosphere, *Global Biogeochem. Cycles*, *6*, 175-183, 1992.

Aneja, V. P., Natural sulfur emissions into the atmosphere, *J. Air Waste Manage. Assoc.*, *40*, 4, 1990.

Ayers, G. P., J. P. Ivey, and R. W. Gillet, Coherence between seasonal cycles of dimethyl sulphide, methanesulphonate and sulphate in marine air, *Nature*, *349*, 404-406, 1991.

Barnard, W. R., M. O. Andreae, W. E. Watkins, H. Bingemer, and H. W. Georgii, The flux of dimethylsulfide from the oceans to the atmosphere, *J. Geophys. Res.*, *87*, 8787-8793, 1982.

Barnes, I., V. Bastian, and K. H. Becker, Kinetics and mechanisms of the reaction of OH radicals with dimethyl sulfide, *Int. J. Chem. Kinet.*, *20*, 415-431, 1988.

Barrie, L. A., and J. M. Hales, The spatial distributions of precipitations acidity and major ion wet deposition in North America during 1980, *Tellus*, *36B*, 333-355, 1984.

Bates, T. S., R. J. Charlson, and R. H. Gammon, Evidence for the climatic role of marine biogenic sulphur, *Nature*, *329*, 319-321, 1987.

Bates, T. S., and J. E. Johnson, Electron capture sulfur measurements of DMS, CS_2 and OCS during CITE-3, *Eos Trans. AGU*, *71*, 1255, 1990a.

Bates, T. S., J. E. Johnson, P. K. Quinn, P. D. Goldan, W. C. Kuster, D. C. Covert, and C. J. Hahn, The biogeochemical sulfur cycle in the marine boundary layer over the Northeast Pacific Ocean, *J. Atmos. Chem.*, *10*, 59-81, 1990b.

Bates, T. S., B. K. Lamb, A. Guenther, J. Dignon, and R. E. Stoiber, Sulfur emissions to the atmosphere from natural sources, *J. Atmos. Chem.*, *14*, 315-357, 1992.

Berresheim, H., Biogenic sulfur emissions from the sub-antarctic and antarctic oceans, *J. Geophys. Res.*, *92*, 13,245-13,262, 1987.

Berresheim, H., M. O. Andreae, G. P. Ayers, R. W. Gillet, J. T. Merrill, V. J. Harris, and W. L. Chameides, Airbone measurements of dimethylsulfide, sulfur dioxide, and aerosols ions over the southern ocean south of Australia, *J. Atmos. Chem.*, *10*, 342-370, 1990.

Berresheim, H., and V. D. Vulcan, Vertical distributions of COS, CS_2, DMS and other sulfur compounds in a loblolly pine forest, *Atmos. Environ.*, *26A*, 2031-2036, 1992.

Bingemer, H. G., M. O. Andreae, T. W. Andreae, P. Artaxo, G. Helas, D. J. Jacob, N. Mihalopoulos, and B. C. Nguyen, Sulphur gases and aerosols in and above the equatorial African rain forest, *J. Geophys. Res.*, *97*, 6207-6217, 1992.

Bluth, G. J. S., S. D. Doiron, C. C. Schnetzler, A. J. Krueger, and L. S. Walter, Global tracking of the SO_2 clouds from the June 1991 Mount Pinatubo eruptions, *Geophys. Res. Lett.*, *19*, 151-154, 1992.

Boatman, J. F., D. L. Wellman, C. C. van Valin, R. L. Gunter, J. D. Ray, H. Sievering, Y. Kim, S. W. Wilkison, and M. Luria, Airbone sampling of selected trace chemicals above the central United States, *J. Geophys. Res.*, *94*, 5081-5093, 1989.

Calvert, J. G., and W. R. Stockwell, Acid generation in the troposphere by gas phase chemistry, *Environ. Sci. Technol.*, *17*, 428-443, 1983.

Calvert, J. G., A. Lazrus, G. L. Kok, B. G. Heikes, J. G. Walega, J. Lind, and C. A. Cantrell, Chemical mechanisms of acid generation in the troposphere, *Nature*, *317*, 27-35, 1985.

Carlier, P., L'ozone serait-il l'oxydant principal du sulfure de diméthyle en milieu océanique, *Atmospheric Ozone*, edited by C. S. Zerefos and A. Ghazi, pp. 815-819, D. Reidel, Norwell, Mass., 1985.

Carroll, M. A., Measurements of OCS and CS_2 in the free troposphere, *J. Geophys. Res.*, *90*, 10,483-10,486, 1985.

Castro, M. S., and J. N. Galloway, A comparison of sulfur free and ambient air enclosure techniques for measuring the exchange of reduced sulfur gases between soils and the atmosphere, *J. Geophys. Res.*, *96*, 15,427-15,437, 1991.

Charlson, R. J., S. E. Schwartz, J. M. Hales, R. D. Cess, J. A. Coakley Jr, J. E. Hansen, and D.J. Hofmann, Climate forcing by anthropogenic aerosols, *Science*, *255*, 423-430, 1992.

Chatfield, R. B., and P. J. Crutzen, Sulfur dioxide in remote oceanic air: Cloud transport of reactive precursors, *J. Geophys. Res.*, *89*, 7111-7132, 1984.

Chatfield, R. B., and P. J. Crutzen, Are there interactions of iodine and sulfur species in marine air photochemistry?, *J. Geophys. Res.*, *95*, 22,319-22,341, 1990.

Chaumerliac, N., E. Richard, J.-P. Pinty, and E. C. Nickerson, Sulfur scavenging in a mesoscale model with quasi-spectral microphysics: Two-dimensional results for continental and maritime clouds, *J. Geophys. Res.*, *87*, 3114-3126, 1987.

Cooper, D. J., and E. S. Saltzman, Measurements of atmospheric dimethyl sulfide and carbon disulfide in the Western Atlantic boundary layer, *J. Atmos. Chem.*, *12*, 153-168, 1991.

Costen R. C., G. M. Tennille, and J. S. Levine, Cloud pumping in a one-dimensional model, *J. Geophys. Res.*, *93*, 15,941-15,954, 1988.

Cullis C. F., and M. M. Hirschler, Atmospheric sulphur: Natural and man-made sources, *Atmos. Environ.*, *14*, 1263-1278, 1980.

Crutzen, P. J., L. E. Heidt, J. P. Krasnec, W. H. Pollock, and W. Seiler, Biomass burning as a source of atmospheric gases CO, H_2, N_2O, NO, CH_3Cl and COS, *Nature*, *282*, 253-256, 1979.

Delmas, R., On the emission of carbon, nitrogen and sulfur in the atmosphere during the bushfires in intertropical savannah zones, *Geophys. Res. Lett.*, *9*, 761-764, 1982.

Delmas, R., and J. Servant, Atmospheric balance of sulfur above an equatorial forest, *Tellus*, *35B*, 110-120, 1983.

Dentener, F. J., and P. J. Crutzen, Reaction of N_2O_5 on tropospheric aerosols: Impact on the global distribution of NO_x, O_3, and OH, *J. Geophys. Res.*, *98*, 7149-7163, 1993.

Eliassen, A., and J. Saltbones, Modelling of long-range transport of sulphur over Europe: A two-year model run and some model experiments, *Atmos. Environ.*, *17*, 1457-1473, 1983.

EMEP (Co-operative Program for Monitoring and Evaluation of the Long Range Transmission of Air Pollutants in Europe), Summary report from the chemical coordinating center for the second phase of EMEP, *EMEP/-CCC Rep. 2-84*, Norw. Inst. for Air Res., Lillestrom, Norway, 1984.

EMEP (Co-operative Program for Monitoring and Evaluation of the Long Range Transmission of Air Pollutants in Europe), Iversen, T., J. Saltbones, H. Sandnes, A. Eliassen, and O. Hov, Airborne transboundary transport of sulphur and nitrogen species over Europe - model descriptions and calculations, *Tech. Rep. 80*, Norw. Meterol. Inst., Oslo, Norway, 1989.

Erickson, D. J. III, J. J. Walton, S. J. Ghan, and J. E. Penner, Three-dimensional modeling of the global atmospheric sulfur cycle: A first step, *Atmos. Environ.*, *25A*, 2513-2520, 1991.

Ferek, R. J., and M. O. Andreae, The supersaturation of

carbonyl sulfide in surface waters of the Pacific Ocean off Peru, *Geophys. Res. Lett.*, *10*, 393-396, 1984.

Ferek, R. J., R. B. Chatfield, and M. O. Andreae, Vertical distribution of dimethylsulfide in the marine atmosphere, *Nature*, *320*, 514-516, 1986.

Galloway, J. N., G. E. Lickens, W. C. Keene, and J. M. Miller, The composition of precipitation in remote areas of the world, *J. Geophys. Res.*, *87*, 8771-8786, 1982.

Galloway, J. N., and A. Gaudry, The composition of precipitation on Amsterdam Island, *Atmos. Environ.*, *18*, 2649-2656, 1984.

Galloway, J. N., The deposition of sulfur and nitrogen from the remote atmosphere, in *The Biogeochemical Cycling of Sulfur and Nitrogen in the Remote Atmosphere* edited by J. N. Galloway, R. J. Charlson, M. O. Andreae and H. Rodhe, pp. 143-176, D. Reidel, Norwell, Mass., 1985.

Galloway, J. N., W. C. Keene, A. A. P. Pszenny, D. M. Whelpdale, H. Sievering, J. T. Merrill, and J. F. Boatman, Sulfur in the western north Atlantic Ocean atmosphere: Results from a summer 1988 ship/aircraft experiments, *Global Biogeochem. Cycles*, *4*, 349-365, 1990.

Georgii, H. W., *Review of the Chemical Composition of Precipitation as Measured by the WMO, BAPMON Global Environmental Monitoring System*, World Meteorol. Org., Geneva, Switzerland, 1982.

Giorgi, F., and W. L. Chameides, Rainout lifetimes of highly soluble aerosols and gases as inferred from simulations with a general circulation model, *J. Geophys. Res.*, *91*, 14,367-14,376, 1986.

Goldan, P. D., W. C. Kuster, D. L. Albritton, and F. C. Fehsenfeld, The measurement of natural sulfur emissions from soils and vegetation: Three sites in the eastern United States revisited, *J. Atmos. Chem.*, *5*, 439-467, 1987.

Guenther, A. B., B. K. Lamb, and H. H. Westberg, U.S. National biogenic sulfur emissions inventory, in Biogenic Sulfur in the Environment, edited by E. S. Saltzman and W. J. Cooper, *Am. Chem. Soc. Symp. Ser. 393*, 14-30, 1989.

Hameed, S., and J. Dignon, Changes in the geographical distributions of global emissions of NO_x and SO_x from fossil-fuel combustion between 1966 and 1980, *Atmos. Environ.*, *22*, 441-449, 1988.

Harvey, G. R., and R. F. Lang, Dimethylsulfoxide and dimethylsulfone in the marine atmosphere, *Geophys. Res. Lett.*, *13*, 49-51, 1986.

Heintzenberg, J., and S. Larssen, SO_2 and SO_4^{2-} in the arctic: Interpretation of observations at three Norwegian arctic-subarctic stations, *Tellus*, *35B*, 255-265, 1983.

Herrmann, J., and W. Jaeschke, Measurements of H_2S and SO_2 over the Atlantic Ocean, *J. Atmos. Chem.*, *1*, 111-123, 1984.

Hoffmann, M. R., and J. O. Edwards, Kinetics of the oxidation of sulfite by hydrogen peroxide in acid solution, *J. Phys. Chem.*, *79*, 2096-2098, 1975.

Hoigné, J., and H. Bader, Rate constants of reactions of ozone with organic and inorganic compounds in water, 2, Dissociating organic compounds, *Water Res.*, *17*, 185-194, 1983.

Hoppel, W. A., Nucleation in the MSA-water vapor system, *Atmos. Environ.*, *21*, 2703-2709, 1987.

Huebert, B. J., S. Howell, P. Laj, J. E. Johnson, T. S. Bates, P. K. Quinn, V. Yegorov, A. D. Clarke, and J. N. Porter, Observations of the atmospheric sulfur cycle on SAGA 3, *J. Geophys. Res.*, *98*, 16,985-16,995, 1993.

Hynes, A. J., P. H. Wine, and D. H. Semmes, Kinetics and mechanism of OH reactions with organic sulfides, *J. Phys. Chem.*, *90*, 4148-4156, 1986.

Iversen T., J. Saltbones, H. Sandnes, A. Eliassen, and O.

Hov, Airborne transboundary transport of sulphur and nitrogen over Europe, model descriptions and calculations, *EMEP (Coop. Prog. for Monitor. and Evalu. of the Long Range Transm. of Air Poll. in Eur.) MSC-W Rep. 2/89*, Oslo, Norway, 1989.

Jaeschke, W., H. Claude, and J. Herrmann, Sources and sinks of atmospheric H_2S, *J. Geophys. Res.*, *85*, 5639-5644, 1980.

Jaecker-Voirol, A., and P. Mirabel, Heteromolecular nucleation in the sulfuric acid-water system, *Atmos. Environ.*, *23*, 2053-2057, 1988.

Johnson, J. E., and H. Harrison, Carbonyl sulfide concentrations in the surface waters and above the Pacific Ocean, *J. Geophys. Res.*, *91* , 7883-7888, 1986.

Junge, C. E., and P. E. Gustafson, On the distribution of sea salt over the United States and its removal by precipitation, *Tellus*, *9*, 164-173, 1957.

Junge, C. E., *Air Chemistry and Radioactivity*, Academic, San Diego, Calif., 1963.

Khalil, M. A. K., and R. A. Rasmussen, Global sources, lifetimes and mass balances of carbonyl sulfide (OCS) and carbon disulfide (CS_2) in the earth's atmosphere, *Atmos. Environ.*, *18*, 1805-1813, 1984.

Kim, K. H., and M. O. Andreae, Carbon disulfide in seawater and the marine atmosphere over the North Atlantic, *J. Geophys. Res.*, *92*, 14,733-14,738, 1987.

Klein, S. A., and D. L. Hartmann, Spurious changes in ISCCP data set, *Geophys. Res. Lett.*, *20*, 455-458, 1993.

Kreidenweis, S., and J. H. Seinfeld, Nucleation of sulfuric acid-water and methanesulfonic acid-water solution particles: Implications for the atmospheric chemistry of organosulfur species, *Atmos. Environ.*, *22* , 283-296, 1988.

Langner, J., and H. Rodhe, A global three-dimensional model of the tropospheric sulfur cycle, *J. Atmos. Chem.*, *13*, 225-263, 1991.

Lazrus, A. L., and B. W. Gandrud, Stratospheric sulfate aerosol, *J. Geophys. Res.*, *79*, 3424-3431, 1974.

Legrand, M., and R. Delmas, The ionic balance of Antarctic snow, a 10-yr detailed record, *Atmos. Environ.*, *18*, 1867-1874, 1984.

Lelieveld, J. The role of clouds in tropospheric photochemistry, *Ph. d. dissertation*, University of Utrecht, The Netherlands, 1990.

Lelieveld, J., and P. J. Crutzen, The role of clouds in tropospheric photochemistry, *J. Atmos. Chem.*, *12*, 229-267, 1991.

Lezberg, E. A., F. M. Humenik, and D. A. Otterson, Sulfate and nitrate mixing ratios in the vicinity of the tropopause, *Atmos. Environ.*, *13*, 1299-1304, 1979.

Likens, G. E., W. C. Keene, J. M. Miller, and J. N. Galloway, The chemistry of precipitation in Katherine, Australia, *J. Geophys. Res.*, *92*, 13,299-13,314, 1987.

Luecken, D. J., C. M. Berkowitz, and R. C. Easter, Use of a three dimensional cloud chemistry model to study the transatlantic transport by soluble sulfur species, *J. Geophys. Res.*, *86*, 22,477-22,490, 1991.

Madronich, S., Photodissociation in the atmosphere, 1, Actinic flux and the effects of ground reflections and clouds, *J. Geophys. Res.*, *92*, 9740-9752, 1987.

Maguin, F., A. Mellouki, G. Laverdet, G. Poulet, and G. Le Bras, Kinetics of the reactions of the IO radical with dimethyl sulfide, methanethiol, ethylene and propylene, *Int. J. Chem. Kinet.*, *23*, 237-245, 1991.

Maroulis, P. J., A. L. Torres, A. B. Goldberg, and A. R. Bandy, Atmospheric SO_2 measurements on project Gametag, *J. Geophys. Res.*, *85*, 7345-7349, 1980.

Martin, L. R., and D. E. Damschen, Aqueous oxidation of sulfur dioxide by hydrogen peroxide at low pH, *Atmos. Environ.*, *16*, 1615-1621, 1981.

Martin, A., Estimated washout coefficients for sulfur dioxide, nitric oxide and ozone, *Atmos. Environ.*, *18*, 1955-1961, 1984.

Meixner, F. X., The vertical sulfur dioxide distribution at the tropopause level, *J. Atmos. Chem.*, *2*, 175-189, 1984.

Mihalopoulos, N., B. Bonsang, B. C. Nguyen, M. Kanakidou and S. Belviso, Field observations of carbonyl sulfide deficit near the ground: Possible implications of vegetation, *Atmos. Environ.*, *23*, 2159-2166, 1989.

Molina, L. T., J. J. Lamb, and M. J. Molina, Temperature dependant UV absorption cross sections for carbonyl sulfide, *Geophys. Res. Lett.*, *8*, 1008-1011, 1981.

Müller, J. F., Geographical distribution and seasonal variation of surface emissions and deposition velocities of atmospheric trace gases, *J. Geophys. Res.*, *97*, 3787-3804, 1992.

Müller, J. F., Modélisation tri-dimensionnelle globale de la chimie et du transport des gaz en trace dans la troposphère, *Aeronom. Acta, A, 370*, 1993.

Müller, J. F., and G. P. Brasseur, IMAGES: A three-dimensional chemical transport model of the global troposphere, in press, *J. Geophys. Res.*, 1994.

Newhall, C. G., and S. Self, The volcanic explosivity index (VEI): An estimate of explosive magnitude for historical volcanism, *J. Geophys. Res.*, *87*, 1231-1238, 1982.

Nguyen, B. C., B. Bonsang, and A. Gaudry, The role of the ocean in the global atmospheric sulfur cycle, *J. Geophys. Res.*, *88*, 10,903-10,914, 1983.

Nguyen, B. C., C. Bergeret, and G. Lambert, Exchange rates of dimethylsulfide between ocean and atmosphere, in *Gas Transfer at Water Surfaces*, edited by W. Brutsaert and G. H. Jirka, pp. 539-545, D. Reidel, Norwell, Mass., 1984.

Nguyen, B. C., S. Belviso, N. Mihalopoulos, J. Gostan, and P. Nival, Dimethyl sulfide production during natural phytoplanktonic blooms, *Mar. Chem.*, *24*, 133-141, 1988.

Nguyen, B. C., N. Mihalopoulos, and S. Belviso, Seasonal variation of atmospheric dimethylsulfide at Amsterdam Island in the Southern Indian Ocean, *J. Atmos. Chem.*, *11*, 123-141, 1990.

Okabe, H., *Photochemistry of Small Molecules*, 217 pp., John Wiley, New York, 1978.

Olson, J. S., J. A. Watts, and L. J. Allison, Major world ecosystem complexes ranked by carbon in live vegetation, a database, *ORNL-5862*, Dep. of Energy, Oak Ridge Natl. Lab., Oak Ridge, Tenn., 1985.

Oort, A. H., Global atmospheric statistics 1958-1973, *NOAA Prof. Pap.*, *14*, U.S. Gov. Print. Off., Wash, D.C., 1983.

Organization for Economic Cooperation and Development (OECD), The OECD Program on long range transport of pollutants, *Summ. Rep.*, Org. for Econom. Coop. and Dev., Paris, 1977.

Organization for Economic Cooperation and Development/International Energy Agency (OECD/IEA), *Quarterly Oil Statistics and Energy Balances, 4th quarter 1988*, Org. for Econom. Coop. and Dev., Paris, 1989.

Penkett, S. A., B. M. R. Jones, K. A. Brice, and A. E. J. Eggleton, The importance of atmospheric ozone and hydrogen peroxide in oxidizing sulphur dioxide in cloud and rainwater, *Atmos. Environ.*, *13*, 123-137, 1979.

Prospero, J. M., D. L. Savoie, E. S. Saltzman, and R. Larsen, Impact of oceanic sources of biogenic sulphur on sulphate aerosol concentrations at Mawson, Antarctica, *Nature*, *350*, 221-223, 1991.

Pszenny, A. A. P., F. McIntyre, and R. A. Duce, Seasalt and the acidity of marine rain on the windward coast of Samoa, *Geophys. Res. Lett.* *9*, 751-754, 1982.

Pszenny, A. A. P., G. R. Harvey, C. J. Brown, R. F. Lang, W. C. Keene, J. N. Galloway, and J. T. Merrill, Measurements of DMS oxidation products in the summer-

time North Atlantic marine boundary layer, *Global Biogeochem. Cycles*, *4*, 367-379, 1990.

Putaud, J. P., N. Mihalopoulos, B. C. Nguyen, J. M. Campin, and S. Belviso, Seasonal variations of atmospheric sulfur dioxide and dimethylsulfide concentrations at Amsterdam Island in the Southern Indian Ocean, *J. Atmos. Chem.*, *15*, 117-131, 1992.

Quinn, P. K., T. S. Bates, J. E. Johnson, D. S. Covert, and R. J. Charlson, Interactions between the sulfur and reduced nitrogen cycles over the central Pacific Ocean, *J. Geophys. Res.*, *95*, 16,405-16,416, 1990.

Rodhe, H., and J. Grandell, On the removing time of aerosol particles from the atmosphere by precipitation scavenging, *Tellus*, *24*, 442-454, 1972.

Rodhe, H., E. Mukolwe, and R. Söderlund, Chemical composition of precipitation in East Africa, *Kenya J. Sci. Technol. Ser. A, 2*, 3-11, 1981.

Rodhe, H., and I. Isaksen, Global distribution of sulfur compounds in the troposphere estimated in a height/latitude transport model, *J. Geophys. Res.*, *85*, 7401-7409, 1980.

Rossow, W. B., L. C. Garder, P. J. Lu, and A. W. Walker, International Satellite Cloud Climatology Project (ISCCP) Documentation on cloud data, *Rep. WMO/TD-266*, 78 pp., World Meteorol. Org., Geneva, 1987.

Saltzman, E. S., D. L. Savoie, J. M. Prospero, and R. G. Zika, Methanesulfonic acid and non-sea-salt sulfate in Pacific air: Regional and seasonal variations, *J. Atmos. Chem.*, *4*, 227-240, 1986.

Saltzman, E. S., and D. J. Cooper, Shipboard measurements of atmospheric dimethylsulfide and hydrogen sulfide in the Carribbean and Gulf of Mexico, *J. Atmos. Chem.*, *7*, 191-209, 1988.

Savoie, D. L., and J. M. Prospero, Comparison of oceanic and continental sources of non-sea-salt sulphate over the Pacific Ocean, *Nature*, *339*, 685-687, 1989.

Savoie, D. L., J. M. Prospero, and E.S. Saltzman, Non-sea-salt sulfate and nitrate in trade wind aerosols at Barbados: Evidence for long-range transport, *J. Geophys. Res.*, *94*, 5069-5080, 1989.

Shaw, R. W. Jr and R. J. Paur, Measurements of sulfur in gases and particles during sixteen months in the Ohio river valley, *Atmos. Environ.*, *17*, 1431-1438, 1983.

Shea, D. J., Climatological atlas: 1950-1979, *NCAR Tech. Note, NCAR/TN-269+STR*, Natl. Cent. Atmos. Res., Boulder, Colo., 1986.

Simkin, T., L. Siebert, L. McClelland, D. Bridge, C. Newhall, and J. H. Latter, *Volcanoes of the World: A Regional Directory, Gazetteer and Chronology of Volcanism During the Last 10000 Years*, Stroudsburg, Pennsylvania, 232 pp., Van Nostrand Reinhold, New York, 1981.

Spiro, P. A., D. J. Jacob, and J. A. Logan, Global inventory of sulfur emissions with 1°x1° resolution, *J. Geophys. Res.*, *97*, 6023-6036, 1992.

Stoiber, R. E., S. N. Williams, and B. Huebert, Annual contribution of sulfur dioxide to the atmosphere by volcanoes, *J. Volcanol. and Geotherm. Res.*, *33*, 1-8, 1987.

Sze, N. D., and M. K. W. Ko, Photochemistry of COS, CS_2, CH_3SCH_3 and H_2S: Implications for the atmospheric sulfur cycle, *Atmos. Environ.*, *14*, 1123-1239, 1980.

Taylor, G. E. Jr., S. B. McLaughlin Jr., D. S. Shriner, and W. J. Selvidge, The flux of sulfur-containing gases to vegetation, *Atmos. Environ.*, *17*, 789-796, 1983.

Thompson, A. M., and R. J. Cicerone, Clouds and wet removal as causes of variability in the trace-gas composition of the marine troposphere, *J. Geophys. Res.*, *87*, 8811-8826, 1982.

Thornton, D. C., A. R. Bandy, and A. R. Driedger III, Sulfur dioxide over the Western Atlantic Ocean, *Global Biogeochem. Cycles*, *1*, 317-328, 1987.

Toon, O. B., J. F. Kasting, P. Turco, and M. S. Liu, The sulfur cycle in the marine atmosphere, *J. Geophys. Res.*, *92*, 943-963, 1987.

Trenberth, K. E., and J. G. Olson, ECMWF Global Analyses 1979-1986: Circulation statistics and data evaluation, *NCAR Tech. Note NCAR/TN-300+STR*, Natl. Cent. Atmos. Res., Boulder, Colo., 1988.

Tucker, B. J., P. J. Maroulis, and A. R. Bandy, Free tropospheric measurements of CS_2 over a 45°N to 45°S latitude range, *Geophy. Res. Lett.*, *12*, 9-11, 1985.

Turco, R. P., and R. C. Whitten, A note on the averaging of aeronomical models, *J. Atmos. Terr. Phys.*, *40*, 13-20, 1978.

Tyndall, G. S., and A. R. Ravishankara, Atmospheric oxidation of reduced sulfur species *Int. J. Chem. Kinet. 23*, 483-527, 1991.

United Nations (UN), *Energy Statistics Yearbook*, United Nations, New York, 1986.

United Nations (UN), Statistiques de l'environnement en Europe et en Amérique du Nord, *Recueil Expérimental, Normes et Études Statistiques, 39*, United Nations, New York, 1988.

Van Valin, C. C., H. Berresheim, M. O. Andreae, and M. Luria, Dimethyl sulfide over the western Atlantic Ocean, *Geophys. Res. Lett.*, *14*, 715-718, 1987.

Varhelyi, G. and G. Gravenhorst, Production rate of airborne sea-salt sulfur deduced from chemical analysis of marine aerosols and precipitation, *J. Geophys. Res.*, *88*, 6737-6751, 1983.

Voldner, E. C., L. A. Barrie, and A. Sirois, A literature review of dry deposition of oxides of sulphur and nitrogen with emphasis on long-range transport modelling in North America, *Atmos. Environ.*, *20*, 2101-2123, 1986.

Walcek, C. J., R. A. Brost, J. S. Chang, and M. L. Wesely, SO_2, sulfate and HNO_3 deposition velocities computed using regional landuse and meteorological data, *Atmos. Environ.*, *20*, 949-964, 1986.

Warneck, P., Chemistry of the natural atmosphere, *International Geophysical Series 41* , 757 pp., Academic, San Diego, Calif., 1987.

Warren S. G., C. J. Hahn, and J. London, Simultaneous occurrence of different cloud types, *J. Clim. Appl. Meteorol.*, *24*, 658-667, 1985.

Watts, S. F., P. Brimblecombe, and A. Watson, Methanesulphonic acid, dimethyl sulphoxide and dimethyl sulphone in aerosols, *Atmos. Environ.*, *24A*, 353-359. 1990.

Yin, F., D. Grosjean, and J. H. Seinfeld, Analysis of atmospheric photooxidation mechanisms for organosulfur compounds, *J. Geophys. Res.*, *91*, 14,417-14,438, 1986.

Zobler, L., A world soil file for global climate modeling, *NASA Tech. Mem.*, *87802*, 32, 1986.

G. P. Brasseur, and C. Granier, National Center for Atmospheric Research, P. O. Box 3000, Boulder, CO 80307. (e-mail: brasseur@brasseur.acd.ucar.edu; granier@granier.acd.ucar.edu)

G. Mégie, and M. Pham, Service d'Aéronomie, Boîte 102, 4 Place Jussieu, 75232 Paris Cedex 05, France. (e-mail: Gerard.Megie@aero.jussieu.fr; Mai.Pham@aero.jussieu.fr)

J.-F. Müller, Belgian Institute for Space Aeronomy, 3 Avenue Circulaire, B-1180 Brussels, Belgium. (e-mail: jfm@atmos.oma.be)